UNIVERSITEIT GENT

Faculteit Wetenschappen
Academiejaar 2010-2011

The Holographic Principle

Jacopo Bono

Promotor: dr. Karel van Acoleyen

Masterproef voorgedragen tot het bekomen van de graad van
Master in de Fysica en Sterrenkunde

UNIVERSITEIT GENT

Faculteit Wetenschappen
Academiejaar 2010-2011

The Holographic Principle

Jacopo Bono

Promotor: dr. Karel van Acoleyen

Masterproef voorgedragen tot het bekomen van de graad van
Master in de Fysica en Sterrenkunde

Acknowledgements

First of all I would like to thank my promotor, Karel van Acoleyen. Not only for the given opportunity to study this remarkable feature of our universe, but certainly also for the help I received during the work and for some interesting discussions about the holographic principle.
I would also like to thank my friends in the second master of physics at the Ghent university, with whom I shared a substantial part of the past five years.
Special thanks to my housemates, for there support and entertainment when needed.
Finally, I thank my parents, my sister and my brother for their care, and especially my father for his frequent questions and conversations about the compelling features of modern physics.

Jacopo Bono
01/09/2011

Contents

Chapter 1

Outline and relevance

During the past decades, a remarkable property was discovered which seemed to be universally valid: breakthroughs in black hole thermodynamics were followed by a new limit on the information content of spacetime, finally leading to the formulation of the holographic principle. This limit is not predicted by any existing theory, and might be a hint of an underlying, more fundamental, and until now unknown theory.
It is that property of our universe that will be studied in this thesis, which is organized as follows: after this introductory chapter, an overview of the holographic principle will be given in Part I, based on the paper 'The holographic principle' by Bousso [1]. In Part II, a study of the paper 'Saturating the holographic entropy bound' [2] will be presented, followed by some original results for anisotropic (Bianchi) and inhomogeneous (LTB) cosmological models in the context of this latter paper.

1.1 Entropy and information

In thermodynamics entropy is interpreted as the amount of distinct microscopic states compatible with a certain macro-state of a system. The statistical calculation of the thermodynamic entropy consists of taking the logarithm of the number of accessible quantum states, i.e. the logarithm of the dimension of the Hilbert space of the system. In information theory, on the other hand, Shannon [3] introduced the Shannon entropy as a measure for the amount of information contained in a system. This Shannon entropy depends on the probability distribution of the variables that form the system, and is expressed in number of bits.

Remarkably, the formula to calculate the Shannon information has the same form as the Boltzmann formula for thermodynamic entropy, which was the first reason while it was called Shannon entropy. It was later discovered that these two entropies are in fact compatible [4, 5]: the thermodynamic entropy of a system is equal to the amount of Shannon information needed to fully describe the microscopic state of that system.
However, some differences between the two entropies appear to be present. Firstly, the

Shannon entropy is expressed in bits, while the thermodynamic entropy is expressed in energy divided by temperature. But this is only a matter of convention and does not invalidate their conceptual equivalence. A second difference is that the thermodynamic entropy is usually a much larger number than Shannon entropy, when expressed in common units. This is due to the fact that, concerning information storage today in e.g. a computer chip, the data is not carried by every atom but by larger components. Hence the contribution to the Shannon entropy comes from the degrees of freedom of the components, while the thermodynamic entropy depends on the state of all the atoms itself, which is a vastly larger amount. If, however, the degrees of freedom in consideration would be the same, we would find the two entropies te be equivalent, and hence the entropy of a system is a quantity that describes the amount of information stored in that system.

1.2 Information content of the fundamental theory

Instead of determining how much information is needed to completely describe a specific system, we could ask a more profound question: how much information is needed, at the most fundamental level, to describe any possible state given only a certain region of spacetime. Thus, we are not searching for the dimension of the Hilbert space of a certain system, but the dimension of the Hilbert space that describes all possible systems. The only limitation is the region of spacetime we are considering. We are then considering the building blocks of the most fundamental theory, hence these building blocks are called the constituents of the *fundamental system* [1]. The amount of information contained in such a fundamental system is therefore an insight on the complexity of our universe at its fundamental level.

However, this fundamental theory is yet unknown and only approximated theories are in use. Suppose for example that local quantum field theory (QFT) would be the fundamental theory. The QFT can be regarded as consisting of harmonic oscillators in every point of space. The dimension of the Hilbert space of such an oscillator is infinite. However, some restrictions have to be made. QFT is a theory describing the world above the Planck scale, and hence we should divide the volume V into Planck volumes, and allowe only one harmonic oscillator per volume. The oscillators would then experience two cut-offs: a low energy cut-off realized by the finite region of space in consideration, and a high energy cut-off at the Planck energy. The latter is implied by the need for gravitational stability: a higher energy in a Planck volume would generate a black hole. QFT would therefore predict V (in Planck units) oscillators, each of which have a finite number of possible states, let's say n. The total number of independent quantum states in V would therefore be $\mathcal{N} = n^V$, and the number of bits of information stored in the system is the logarithm of this last equation,

$$N = V \ln n \tag{1.1}$$

We see that the amount of information grows with the volume. This is what one would intuitively expect: the bigger the volume, the more information storage is possible, proportional to that volume itself. According to the holographic principle, however, such a fundamental system can be described with substantially less information, proving this intuitive result wrong. This discrepancy can be explained by noticing that the QFT fails to account for all the gravitational effects. Although we required gravitational stability on the Planck scale, if we would assume one Planck mass per Planck volume, this would result in $M \sim R^3$ on a bigger scale, which shows that the system is gravitationally unstable.

The formulation of the holographic principle followed after the proposal of a new limit on the entropy content of a spacetime. In short, the holographic principle states it is the area A of a surface that constrains the amount of information in the bordering regions, and not the volume. The holographic principle therefore relates information and geometry, and this suggests it's origin must lie in a theory which unifies matter and spacetime. It is therefore possible that holographic principle is a property of a not yet discovered more fundamental theory, a quantum theory of gravity.

1.3 Conventions

Throughout the rest of this thesis, we will use Planck units: $\hbar = G = c = k = 1$. All areas are expressed in multiples of the square planck length, $l_P^2 = \frac{G\hbar}{c^3} = 2.59 \times 10^{-66}\text{cm}^2$.
Furthermore, we require the null energy condition and the causal energy condition on the stress tensor, T_{ab}, to hold for a physically realistic system. A definition of these conditions and other terms that will be used can be found in appendix A.

Part I

Towards a holographic principle

Chapter 2

The origin of entropy bounds

As stated in the previous chapter, the holographic principle is not predicted by currently existing theories. Instead, it's origin lies in the entropy bounds that emerged as a consequence of studying black hole in a thermodynamic context. The next paragraphs will therefore be dedicated to a brief historical overview of black hole thermodynamics and its implications, especially the merit of the work of Hawking and Bekenstein. For a more detailed look into their work and that of others, we refer to the literature.

2.1 Black hole thermodynamics

Black hole thermodynamics started when an analogy was discovered between some black hole properties and thermodynamic entropy. The first property we consider is that the area of a black hole event horizon never decreases with time. If two black holes merge, the area of the new black hole will exceed the total area of the original black holes. This is called the area theorem. A second property is that a stationary black hole is characterized by only three quantities: mass, angular momentum and charge. A complex system collapsing to form a black hole will therefore result in a unique stationary state, which is the so-called the no-hair theorem.

The latter theorem, however, has an important consequence. A collapsing system may have arbitrary large entropy, while the final state has none at all. It seems that, at least for an outside observer, the second law of thermodynamics is violated. Bekenstein showed that dropping matter into an existing black hole results in a similar problem. Since different initial conditions can lead to the same indistinguishable final state, this would result in a loss of information. However, the area theorem states that the area of the event horizon will grow. Bekenstein solved this apparent paradox by suggesting that the black hole carries an entropy equal to its horizon area, $S_{BH} = \eta A$. The number η will later be determined to be $\frac{1}{4}$,

$$S_{BH} = \frac{1}{4}A \tag{2.1}$$

Let us remark that the microscopic origin of this entropy is not yet well understood: classically the black hole carries no entropy, while the Bekenstein-Hawking formula (2.1) predicts that it is compatible with $e^{S_{BH}}$ quantum states.

2.2 Generalized second law

In order to solve the problem encountered using the second law of thermodynamics, Bekenstein suggested a modified version that still holds for gravitational collapse of matter in black holes. The generalized second law of thermodynamics (GSL) states that it is the sum of ordinary matter entropy and black hole entropy that will never decrease,

$$dS_{total} = dS_{matter} + dS_{BH} \geq 0. \tag{2.2}$$

One could still wonder if this black hole entropy is just a mere analogy between black holes and thermodynamics, or if black holes are indeed to be considered as thermodynamic objects. If the latter is the case, then the first law of thermodynamics would predict that black holes have a temperature. Indeed, if we consider a black hole to be a thermodynamic system with mass M and entropy S_{BH}, it should obey the first law

$$\mathrm{d}M = T\mathrm{d}S_{BH}, \tag{2.3}$$

and therefore have a temperature T. This was confirmed by Hawking, when he discovered that a black hole radiates through quantum processes. Furthermore, it was shown that an observer would detect a thermal spectrum at a temperature equal to

$$T = \frac{\kappa}{2\pi}, \tag{2.4}$$

where κ is the surface gravity of the black hole. Comparing this equation to

$$dM = \frac{\kappa}{8\pi} dA. \tag{2.5}$$

derived by Bardeen, Carter and Hawking, and with a clear analogy to the first law of thermodynamics (2.3), one can see that the surface gravity of the black hole plays the role of its temperature and the entropy of the black hole is the horizon area. Likewise, the comparison of the last three equations fixes the coefficient η in Bekensteins formula to be 1/4. The discovery of black hole radiation thus confirmed that a black hole is to be considered as a true thermodynamic object. The next step is to test if the GSL holds for the several new processes involving black holes.

2.2.1 Bekenstein Bound

First, let's consider the case of ordinary matter dropped into a black hole. It is clear that ordinary matter entropy is lost in this process, since S_{matter} starts finite and ends zero.

However, the black hole area, and thus its entropy, will increase. To check if the GSL holds, we need to verify if the following inequality is not violated:

$$S_{matter}^{init} + S_{BH}^{init} \leq S_{BH}^{final}. \tag{2.6}$$

This is the moment where a very interesting property is revealed. Since the amount of area increase of the black hole, hence the increase in black hole entropy, depends on the mass added and not on the entropy of the matter system, the validity of equation (2.6) requires an extra condition on the energy-entropy relation of a system. To see why, let's consider a system that, for a given mass and size, possesses an arbitrarily large amount of entropy. In this way, we can make the entropy loss during the process arbitrarily large, while the entropy gain remains small. Hence this would violate the GSL. However, all the previous considerations about black hole thermodynamics make us confident that we can demand the GSL to hold in all processes, thus considering it as a law of nature. To invalidate our previous argument, we must somehow forbid the possibility for a matter system with fixed mass and size to have arbitrary large entropy. We would have to introduce a universal entropy bound on matter systems, in terms of there extensive parameters. In the next paragraphs, we will find such a bounds by applying the GSL for different processes.

Bekenstein imposed such a bound for weakly gravitating matter systems in asymptotically flat space:

$$S_{matter} \leq 2\pi ER, \tag{2.7}$$

where E is the total mass energy, and R is the radius of the smallest sphere that fits around the system. One can readily see that for spacetime regions for which the gravitation effects become very important, this bound would fail. Indeed, to define R in a highly curved space would lead to trouble. A spherical symmetric system, however, would not encounter this problem. Considering a Schwarzschild black hole in four dimensions, for which we have $R = 2E$, its Bekenstein entropy $S = A/4 = \pi R^2$ exactly saturates the Bekenstein bound. The validity of the Bekenstein bound remains somewhat uncertain, and we refer the interested reader to the literature for more detailed arguments concerning this bound.

2.2.2 Spherical Entropy Bound

Another interesting bound arises when studying the Susskind process. This is the process where matter is converted into a black hole. Suppose we have a matter system of mass E and entropy S_{matter}, in a spacetime $\mathcal{M}$. We then make the following requirements:

1. The asymptotic structure of $\mathcal{M}$ permits the formation of black holes (we will assume asymptotical flatness).

2. In order to be able to define a circumscribing sphere (i.e. the smallest sphere that fits around system), the metric near the system is at least approximately spherically sym-

metric, which is the case for all spherically symmetric systems and all weakly gravitating systems.

3. The matter system is stable on a large timescale, such that the time dependence of A is negligible.

4. The mass of the system is smaller than the mass M of a black hole of the same area (otherwise, the system would not be gravitationally stable and would be already a black hole from the outside point of view).

Here we defined A as the area of the circumscribing sphere. To convert the system into a black hole, we consider a shell of mass $M - E$ and let it collapse onto the matter system. We start with the shell far from the system, and its entropy, S_{shell} is non negative. We therefore have an initial total entropy equal to $S^{initial} = S_{matter} + S_{shell}$. The final state, after the collapsing, is just a black hole with entropy $S^{final} = S_{BH} = \frac{A}{4}$. The GSL in this case leads to

$$S_{matter} \leq A/4, \tag{2.8}$$

since $S_{matter} \leq S^{initial} \leq S^{final} = A/4$. We call this bound the spherical entropy bound. Equation (2.8) would also be the result if we would assume the Bekenstein bound to hold for strongly gravitating systems. In four dimensions, the requirement for gravitational stability is $2M \leq R$. It follows easily from equation (2.7) that $S \leq 2\pi MR \leq \pi R^2 = A/4$. Hence, we showed that the spherical entropy bound is weaker than the Bekenstein bound, when both can be applied. However, the spherical entropy bound is more closely related to the holographic principle, as we will later see.

Examples

The spherical entropy bound can be tested for several examples in 4 dimensions.

1. Black Holes
The entropy of a single Schwarzschild black hole exactly saturates the bound: $S_{BH} = A/4$. Hence a black hole is the most entropic object one can put inside a given spherical surface.
Secondly, let's consider a system of several black holes of masses M_i. The total entropy of the system is $S = 4\pi \sum M_i^2$. For this system to be observable from an outside viewpoint, the system should not already be a larger black hole of mass $\sum M_i$. The circumscribing spherical area then satisfies:

$$A \geq 16\pi \left(\sum M_i\right)^2 > 16\pi \sum M_i^2 = 4S \tag{2.9}$$

Again, the spherical entropy bound is satisfied.

2. Ordinary matter
If we consider systems that include only ordinary matter, it seems difficult to even approach

saturation. The best option to maximize the entropy, is to consider massless particles: a rest mass would only cause the gravitational instability to grow without contributing to the entropy. Hence we consider a gas of radiation, at temperature T and with energy E, confined inside sphere of radius R. The condition for gravitational stability is, once again, $R \geq 2E$. Furthermore, we neglect self-gravity and consider the system to be embedded in a flat background. The energy of the ball is related to its temperature:

$$E \sim ZR^3T^4 \tag{2.10}$$

Z is number of species of particles in the gas. The entropy of the gas is

$$S \sim ZR^3T^3 \tag{2.11}$$

Combining equations (2.10) and (2.11) we find a relation between entropy, size and energy:

$$S \sim Z^{1/4}R^{3/4}T^{3/4} \tag{2.12}$$

Gravitational stability $R \geq 2E$ implies:

$$S \lesssim Z^{1/4}A^{3/4} \tag{2.13}$$

Since we are working with Planck units, any geometric description about some system can be valid only if the system is (much) bigger than the Planck scale, $A \gg 1$. An estimate of the number of species in nature is $Z \sim O(10^3)$. Hence, equation (2.13) implies the spherical entropy bound (2.8), except for the near-Planck size systems which cannot be adequately described by our approximation.

The Species Problem

From equation (2.13) follows that the spherical entropy bound could be violated if $Z \gtrsim A$. Of course, the number of species in nature is fixed. One can thus wonder if the GSL, from which we derived the spherical entropy bound, could be used to rule out an exponentially large number of species in nature.

Wald showed that, starting from the GSL, one cannot rule out a large number of species. However, in his analysis another criterion against a large number of species is found. Exponentially large Z would lead to unstable black holes, provided they are larger than the Planck scale. If one assumes that at least metastable black holes above the planck scale are possible, then the number of species can never be large enough to contradict equation (2.8).

2.3 Unitarity

The spherical entropy bound showed that any possible system within in a sphere of area A can be described by $A/4$ degrees of freedom, as long as the space is asymptotically flat.

We argued earlier that a local field theory would predict much more degrees of freedom. However, exciting those degrees of freedom would lead to gravitational collapse, resulting in the formation of a black hole. One could then consider this gravitational collapse as a practical limit, but not a fundamental limit on the degrees of freedom. This would leave the possibility of exciting all the degrees of freedom predicted by quantum field theory, but to verify there existence one would need to fall into the black hole.

This consideration can be rejected by the following arguments. The first argument states that a fundamental theory should not contain more elements than it needs to fully describe every possible state. If one can describe all possible physics contained in a spacetime region with $A/4$ degrees of freedom, than one should not use more in the fundamental theory. A more convincing argument follows from the fact that any quantum-mechanical evolution should preserve information, a property which is called unitarity. Suppose a spacetime region is described by a hilbert space of dimension e^V, and suppose this region evolves into a black hole. From the Bekenstein entropy, we would find that now this region is described by a Hilbert space of dimension $e^{A/4}$. This is a decrease in number of states, and it would be impossible to recover the initial state from the final, hence violating our unitarity argument.

2.3.1 Black Hole Complementarity

To accept this last argument, one should first prove that unitarity is indeed preserved when including black hole processes. At first, Hawking showed in semiclassical calculations that Hawking radiation is purely thermal, and no information about the ingoing state is present. He therefore claimed that the evaporation of a black hole is not a unitary process. However, one could also argue that unitarity should be preserved in a complete quantum gravity theory, and it is only because this theory is yet unknown that the origin of information in Hawking radiation is not yet understood.

If we insist on unitarity, and therefore assume Hawking radiation to carry information, we encounter another paradox. If the evaporation process is indeed a unitary one, there would seem to be two copies of the same information: one inside the black hole (i.e. the matter system that collapsed) and one outside (i.e. the Hawking radiation). This is a violation of the linearity of quantum mechanics, which forbids the cloning of information. The solution to this paradox is found by noticing that an observer can never retrieve both copies of information. Obviously, an observer in the black hole cannot observe the information from Hawking radiation, and an outside observer cannot collect the information from inside the black hole. Even the case where an observer would retrieve one bit of information outside, and consequently jump into the black hole to observe the same bit of information seems impossible. The observer has to stay outside for a time compared to the evaporation time scale of the black hole in order to collect one bit from the Hawking radiation, and therefore it

becomes impossible to detect the second copy inside. Hence, the paradox can be explained if we assume that there are two complementary descriptions, one for an outside observer and one for an in-falling observer.

If we insist on unitarity, even for processes involving black holes, we can interpret equation (2.8) as follows ('t Hooft(1993), Susskind (1995):

A region with boundary of area A is fully described by no more than A/4 degrees of freedom, or about 1 bit of information per Planck area. A fundamental theory, unlike local field theory, should incorporate this counterintuitive result.

Of course, one should remark that this formulation is obtained from an entropy bound that is not universal.

Chapter 3

Covariant entropy bound

In the previous chapter, we witnessed how the generalized second law of thermodynamics (GSL) arose as a consequence of black hole thermodynamics. When considering several physical processes, imposing this law led to some upper bounds on the amount of entropy in a region of space: the Bekenstein bound and the spherical entropy bound. However, none of those bounds is universal. Both are valid under certain conditions, but counterexamples can be found otherwise. The goal of this chapter will be to find a universal and covariant bound, valid for every region in a spacetime.

3.1 Spacelike entropy bound

A naive attempt in finding a generalized bound, is to forget all about the assumptions made for the spherical entropy bound. Hence, the entropy inside any spacelike region will not exceed the area of the region's boundary. More precisely [1]:
Let V be a compact portion of a hypersurface of equal time in the spacetime $\mathcal{M}$. Let $S(V)$ be the entropy of all matter systems in V. Let B be the boundary of V and let A be the area of the boundary of V. Then

$$S(V) \leq \frac{A[B(V)]}{4} \tag{3.1}$$

We will call this bound the spacelike entropy bound.

It is not difficult to find counterexamples to the spacelike entropy bound. We will now present some of them.

1. Closed spaces

Imagine that a spacetime $\mathcal{M}$ contains a closed spacelike hypersurface $\mathcal{V}$. Lets consider a matter system inside $\mathcal{V}$ occupying a hypersurface $V < \mathcal{V}$. The region Q outside the matter system but within $\mathcal{V}$ has then the same boundary as the region $V = \mathcal{V} - Q$. The area of

this boundary can be made arbitrarily small, by contracting Q to one point. One would then obtain $S_{matter}(V) > A[B(V)]$, which violates the spacelike entropy bound (3.1).

2. Large scale universe

Consider a large scale universe, that is 3-dimensional, isotropic and homogeneous, flat and expanding in time. One can then approximate the entropy content of the universe with an entropy density σ. Next, consider a hypersurface of equal time $\mathcal{V}$. Since we assumed a flat universe, the volume of this hypersurface will be $V = 4\pi R^3/3$, and the area of the corresponding surface $B(V)$ will be $A[B(V)] = 4\pi R^2$. The entropy in the volume is obviously given by $S_{matter}(V) = \sigma V = \frac{\sigma}{6\sqrt{\pi}} A^{3/2}$. It is clear that choosing a large enough radius, $R \geq \frac{3}{4\sigma}$, will lead to a violation of the spacelike entropy bound (3.1).

3. Collapsing star

As a third counterexample, imagine following a collapsing star through its own horizon. The area will then shrink to zero when a star ends in the singularity, but by the GSL the entropy has to be at least S_0, the entropy of the star before the collapse.

4. Weakly gravitating system

Consider a system that satisfies the restrictions imposed by the spherical entropy bound. The system will then be weakly gravitating and spherical, in a flat space. Imagine a special time-slicing for which a hypersurface of constant time is rippled. The boundary of a volume V in this time-coordinate system is the intersection of the rippled hypersurface with the boundary of the world volume of V, and can be made arbitrarily small in this manner: imagine making the boundary null almost everywhere, then the Lorentz contracted surface would be $A\sqrt{1-\beta^2}$, with $\beta \to 1$. This example would even violate the spherical entropy bound, irrespective of the assumptions we made at the start. This apparent discrepancy is explained by noticing that the spacelike bound is not covariant. Depending on the used coordinate system, it can be violated.

3.2 Light-sheets

The key point in defining a covariant version of the spacelike entropy bound, is to find a covariant hypersurface bordering a surface, on which the entropy will be counted. These special types of hypersurfaces will be called light-sheets. In order to specify this 'covariant entropy bound', a good understanding of these light-sheets is needed. The next section will therefore be dedicated to those objects.

3.2.1 Construction

Light-sheets are null hypersurfaces with negative or vanishing expansion, generated by a null congruence of geodesics orthogonal to a surface. Every surface B has exactly four orthogonal null directions. They are commonly called future directed ingoing, future directed outgoing, past directed ingoing and past directed outgoing. Each direction can be used to build a null congruence: starting on the surface, one can follow past and future directed light rays orthogonal to B, on either side. It is due to the Lorentzian geometry that there are precisely four null hypersurfaces orthogonal to B. As we will see, at least two of the four null congruences will be light sheets, as dictated by the condition of none-positive expansion. For a more detailed definition of hypersurfaces and geodesic congruences, we refer to the appendices B and C.

First of all, we want to generalize the notion of inside, when considering a surface B. It is obvious that a given surface cannot be related to the entropy of the infinite 'outside' region. In a closed universe, for example, one should consider only the small three-sphere for a given two-sphere B. In Euclidian space, the contraction criterion defines the notion of 'inside': consider a closed surface in flat Euclidian space, and suppose it's area is A. Next, all the geodesics orthogonal to this surface are constructed. Finally, each of the geodesics is followed a infinitesimal proper distance $d\lambda$, on both sides of the surface. The points will now form a new surface, and the side on which the new surface is smaller than A, is called the inside. This contraction criterion has the advantage of being local, and hence no further information is needed on the surface or the space it is enclosed in.

Some modifications are needed if we want to generalize this contraction condition for Lorentzian geometry. There are an infinite amount of spacelike hypersurfaces containing a surface B, hence the side having a contracting area is dependent on the choice of such a hypersurface. Instead, let's consider the four unique null directions F_i orthogonal to B. The contraction criterion can now be applied along those directions,

- Use the affine parameter λ along the light ray.
- Pick a direction F_i, follow the null geodesics away from B for infinitesimal affine distance $d\lambda$.
- Compare the new constructed surface A' with the original one. If $A' < A$, then direction F_i is an 'inside' direction.

Because opposite pairs of null directions are continuations of each other, at least one of each pair will be inside-directed. Mathematically, the contraction condition is defined in the following way:

$$\theta(\lambda) \leq 0 \qquad \text{for } \lambda = \lambda_0 \tag{3.2}$$

where λ is the affine parameter for light rays generating F_i and we assume λ is increasing in direction away from B. λ_0 is value of λ on B, and θ is the expansion of the null congruence. Another way to define the expansion is

$$\theta(\lambda) \equiv \frac{d\mathcal{A}/d\lambda}{\mathcal{A}} \tag{3.3}$$

where $\mathcal{A}$ is a surface area spanned by light-rays. The locality of the contraction condition has as a consequence that it can be applied to open as well as closed surfaces. Moreover, when the sign of the expansion would change in different parts of a surface, this surface can be split up and the criterion can be applied to each part separately. A surface with both light-sheets on the same spatial side, are called normal. If, on the other hand, a surface has two passed directed light-sheets, it will be called anti-trapped. This can be the case when the expansion (or contraction) of space itself becomes dominant over the expansion of light rays. An expanding universe, for example, will have decreasing surface areas towards the past, since the big bang is approached. If the initial sphere is big enough, both light-sheets will be past directed. Also the opposite is possible, where a surface has two future directed light-sheets. In this case, the surface is called trapped.

3.2.2 Termination

We have now determined a Lorentzian version of the contraction condition. However, we can encounter one more problem. Considering a spherical surface, for example, then the contraction condition implies the light-sheets to be cones bounded by B. However, a restriction is needed to prevent from continuing the light-sheet after the tip of the cone, since the light-sheet would grow infinite after that point. Therefore, we demand the expansion to be non-positive everywhere on the light-sheet, and not only near B. Hence,

$$\theta(\lambda) \leq 0 \tag{3.4}$$

for all values of λ.

Raychaudhuri's equation describes the rate of change of the expansion along the light rays. The equation (3.5) is a generalized version of (C.18) for a D-dimensional spacetime.

$$\frac{d\theta}{d\lambda} = -\frac{1}{D-2}\theta^2 - \sigma_{ab}\sigma^{ab} + \omega_{ab}\omega^{ab} - 8\pi T_{ab}k^a k^b \tag{3.5}$$

where we used the expansion θ, the *shear* σ_{ab}, the *twist* ω_{ab} and the null extrinsic curvature B_{ab}. For suface orthogonal light rays, the twist vanishes. Since we assumed the null energy condition, the last term in equation (3.5) will be non-positive. The right hand side of equation (3.5) will therefore be non-positive for all light sheets. We can then solve the following

inequality,

$$\begin{aligned}
&\frac{d\theta}{d\lambda} \leq -\frac{1}{D-2}\theta^2 \\
\Rightarrow &(D-2)\int_{\theta_1}^{\theta_2}\frac{d\theta}{\theta^2} \geq \int_{\lambda_1}^{\lambda_2} d\lambda \\
\Rightarrow &\frac{D-2}{\theta_2} - \frac{D-1}{\theta_2} \geq \lambda_2 - \lambda_1
\end{aligned} \tag{3.6}$$

From this equation, it follows that if we start with some negative expansion θ_1, then the expansion will diverge to $-\infty$ at some affine parameter λ_2, as shown by

$$\lambda_2 \leq \lambda_1 + \frac{D-2}{|\theta_1|} \tag{3.7}$$

This is called the focussing theorem. As we can now see from equation (3.3), the divergence of the expansion tells us the cross-sectional area is vanishing and we therefore have a encountered a place were infinitesimally neighboring light rays cross each other, which is called a caustic.

By construction the expansion is initially negative or zero on every light-sheet. The focussing theorem guarantees that the expansion can only decrease, and hence equation (3.4) implies that light sheets end at caustics. However, not all light rays need to intersect at the same point to have a positive expansion. In the most general case, each light ray has a different caustic point, leading to very complicated caustic surfaces. Furthermore, non-local intersections of light rays do not lead to violations of the contraction condition. In the case of zero expansion, the focussing theorem cannot be applied and the light sheet will be infinitely large. This will be possible in a flat spacetime without matter or gravitational waves, hence a pure Minkowski spacetime. The light sheet cannot contain any entropy in this case, and the covariant entropy bound is still satisfied.

If such a light sheet does encounter matter, the last term in equation (3.5), $-8\pi T_{ab}k^a k^b$, will become negative. Hence, the light rays will be focussed due to the focussing theorem and they will eventually end in caustics. We can conclude this section by summarizing that one simple condition is obtained which determines both the direction and the extent of light-sheets, equation (3.4).

3.3 Covariant entropy bound and holographic principle

We are now well equipped to make another attempt in finding a covariant generalization of the spacelike entropy bound. The spacelike entropy bound can schematically be written as

1. Start from a spacelike volume V.
2. Find the boundary $B = \partial V$.

3. The area $A(B)$ is an upper limit on the entropy contained in the volume, $S(V)$.

In the covariant case, we reverse this process:

1. Start from a codimension 2 surface B to find a codimension 1 region L.
2. L is a light-sheet, constructed by following light rays orthogonal to the surface B, as long as they are not expanding.

We can than formulate the Covariant Entropy Bound (CEB) [1]:
The entropy on any light-sheet of a surface B will not exceed the area of B:

$$S[L(B)] \leq \frac{A(B)}{4} \tag{3.8}$$

Of course, we have not presented a real derivation for the covariant entropy bound. However, it is clearly covariant and the geometric is well-defined. This arguments and the fact that no counterexample is found so far, strengthens our confidence in the bound.

3.3.1 Dynamics

Now that we have defined the CEB, we would like to gain some more insight in the mechanism underlying the existence of such a universal bound. Since light sheets were one of the key features in order to formulate the covariant entropy bound, it is clear that understanding their dynamical behavior will give us more insight on the bound.

Consider a light-sheet L that contains an amount of entropy equal to S. The entropy on the light-sheet requires the presence of energy, which in turn leads to the focussing of light rays, as can be seen from the Raychaudhuri equation (3.5). As predicted by the focussing theorem, such light-rays will eventually form caustics and the light-sheet will be terminated. More energy would lead to a quicker termination of the light-sheet, hence in order to satisfy the CEB, the relation between entropy and energy is the key. However, a system with the same amount of energy can have different entropy, depending on the microscopic details of the system. The generality of the CEB is therefore even more impressive.

3.3.2 FMW theorems

In some situations, the entropy can be approximated by an entropy density, and hence some general relations can be found between the entropy and energy. Under some assumptions, Flanegan, Marolf and Wald (FMW) showed that the CEB is always satisfied. Only one feature of the FMW theorems will be reviewed, for more details the reader is referred to the literature. This feature is a consequence of the second FMW theorem, and comprises a stronger version of the CEB. Instead of terminating the light sheets only when the expansion becomes positive,

one can terminate the light sheet everywhere. Suppose we follow the generating light rays of a light sheet in the direction of negative expansion starting from a surface A, and stop at a surface $A' < A$. From the second FMW theorem, it then follows that the entropy on this light sheet will not exceed the difference of the area's,

$$S(L) \leq \frac{A - A'}{4} \tag{3.9}$$

It is clear that equation (3.9) generalizes the covariant entropy bound: if we would follow the light rays to a caustic, A' vanishes and the original covariant entropy bound (3.8) is found.

3.3.3 Limitations

Suppose that we would allow matter with negative energy in our fundamental theory. Combining such matter with ordinary (positive energy) matter in a fixed region of space, could create a system with vanishing total energy but arbitrarily large entropy. One could than keep adding matter without gravitational collapse. The geometry would remain flat and the entropy would eventually exceed the area of the surface bounding the region. However, matter with negative mass does not exist in nature, to a good approximation. And since the CEB is a property of nature, we don't want to test its validity with unphysical systems. Therefore, we want to exclude matter who's energy density appears negative to a light ray, or which permits the transport of energy at a speed exceeding that of light. We demand, in other words, the null as well as the causal energy condition. Quantum fluctuations can violate these energy conditions, but a counterexample to the CEB using quantum effects in ordinary matter systems has not yet been found.

Secondly, let's investigate if the quantum fluctuations of the geometry itself could cause violations of the covariant entropy bound. To properly define the bound, we made use of several geometric concepts such as area, orthogonal light rays, etc. Those concepts can only be applied in approximately classical spacetimes, by which we mean large distances compared to the Planck constant $\hbar$ and low curvature. This does not mean its relation with quantum gravity is invalidated, since it still relates the information content of spacetime to its geometry. If one would set $\hbar$ to zero, the bound would not only be unphysical, but it would also be trivially valid since $\frac{Akc^3}{4G\hbar}$ would be infinite.

3.3.4 Spacelike projection theorem

Starting from the CEB, we can now try and find more specialized bounds, which are valid under certain specific assumptions. The spacelike projection theorem provides us with conditions for which the CEB implies the spacelike entropy bound[6]:
Let B be a closed surface. Assume that B permits at least one future directed light sheet L. Moreover, assume that L is complete, i.e. B is its only boundary. Let $S(V)$ be the entropy

in a spatial region V enclosed by B on the same side as L. Then

$$S(V) \leq S(L) \leq A/4 \tag{3.10}$$

The previous theorem can be proven as follows. All matter which is present on V will pass through L, independently of the choice of V (which is dependent on the time slicing we choose). Then the second law of thermodynamics implies the first inequality, and the covariant entropy bound implies the second one. The spacelike projection theorem is only valid in a regime of weak gravitation. We can motivate this by the following two arguments. First of all, if the surface B would not have a future directed light sheet, it would be anti-trapped, which indicates strong gravity. Secondly, if the light sheet L would have other boundaries besides B, this would imply the presence of future singularities close enough to B to end the light sheet. Again, this is a sign of strong gravity. The spacelike projection theorem should thus be used for a closed, weakly gravitating smooth surface. Also the spherical entropy bound can be retrieved from the covariant bound: indeed, under the conditions of section (2.2.2), the conditions for the spacelike projection theorem are satisfied. It was exactly the spherical entropy bound that we used to prove the validity of the GSL in the Susskind process, and the covariant entropy bound thus implies the GSL for the black hole formation processes.

3.4 The Holographic Principle

Since we did not derive the CEB from some theory, we will summarize our motivations for claiming that it is a true property of nature. First of all, the covariant entropy bound is well-defined and testable. The light sheet construction is covariant and the only limit on the bound we have found is that it shouldn't be applied outside the range of semi-classical gravity. But this is precisely the theory we will use, that is until a quantum theory of gravity is available. Furthermore, no counterexample has yet been found. The bound refers to statistical entropy, and since no further assumptions on the microscopic state of the system is made, it puts a fundamental limit on the degrees of freedom in nature. The CEB is non-trivial and differs from its non-universal predecessors, because it surpasses being a mere consequence of black hole thermodynamics. Moreover, since it is not explained by the known laws of physics, it can be regarded as a property of a more fundamental, undiscovered, theory. Since the bound involves the quantum states of a matter system, this fundamental theory should unify matter, gravity and quantum mechanics.

We thus conclude that the area of any surface B determines the information content of an underlying theory describing all possible physics on the light sheet of B. The holographic principle[6, 7] can then be formulated as

The covariant entropy bound is a law of physics which must be manifest in an underlying theory. This theory must be a unified quantum theory of matter and spacetime. From it,

Lorentzian geometries and their matter content must emerge in such a way that the number of independent quantum states describing the light sheets of any surface B is manifestly bounded by the exponential of the surface area:

$$\mathcal{N}\left[L(B)\right] \leq e^{A(B)/4} \tag{3.11}$$

In quantum theory, the logarithm of the dimension $\mathcal{N}$ of the Hilbert space and the amount of information stored in the quantum system are equivalent. Since we don't know if quantum mechanics will be primary in a unified theory, we can also formulate the holographic principle in terms of the number of degrees of freedom instead of the quantum states:

N, the number of degrees of freedom (or the number of bits times $\ln 2$) involved in the description of $L(B)$, must not exceed $A(B)/4$.

Remarks on the holographic principle

The holographic principle predicts a much smaller amount of degrees of freedom than the theories known to date. To our approximation, however, physics appear to be local. How can we formulate a theory in which the covariant entropy bound is manifest, and hence by the holographic principle the information content is not local, yet in approximation the locality resurfaces? Two different approaches are followed in order to find a solution to this apparent contradiction.

The first type of approach is to hold on to a local theory, and introduce an explicit gauge invariance in the theory. The gauge invariance should then leave only as many physical degrees of freedom as dictated by the covariant entropy bound. The difficulty in this approach is obviously to find such a gauge invariance. The second type of approach abandons locality, but instead starts from the holographic principle as the main property. The challenge in this approach lies in understanding and describing the evolution of such a new point of view, and to explain how it can be approximated by a quantum field theory in a classical spacetime under suitable assumptions.

3.5 Holographic screens

An important implication of the holographic principle is that all the information in a given region can be encoded on a surface B, at a density of one bit per Planck area. We can now ask ourselves if the information contained in an entire spacetime can be encoded on a certain hypersurface, which we will call a screen.
A surface B will constrain the amount of information on light sheets generated by light rays starting on every point of B. To find screens, on the other hand, one has to start by following the generating null geodesics of a light sheet in the opposite direction (the direction

of non-negative expansion). If the expansion becomes negative, one has to stop, but there's no restriction from stopping even earlier. The latter procedure is called projection, and the surface where the projection ends is called the screen of the projection. If the expansion vanishes everywhere on the screen, it is called a preferred screen.
In the case of an entire space-time instead of a surface, we will start by slicing the space-time into a one parameter family of null hypersurfaces. The projection along those hypersurfaces will lead to different one parameter families of (D-2) dimensional screens. Each of those families will form a (D-1) dimensional hypersurface of screens, which we will also refer to simply as screen, since it will be clear from the context whether we mean a (D-2) dimensional screen or a screen-hypersurface of a (part of a) spacetime. The latter ones can be either timelike, null or spacelike. A special case is possible if the conditions for the spacelike projection theorem are satisfied: one can than project the information of a spatial region onto a screen along spacelike hypersurfaces.

Considering spherically symmetric metrics, the strategy to find such screens is to choose the light cones centered around $r = 0$ to slice up the spacetime into a family of null hypersurfaces. As a parameter for this family we can use time, thus finding two inequivalent projections, along past directed and along future directed light cones. The following steps should be taken into account to obtain the screen(s) for a spacetime [6]: firstly, a conformal diagram of the spacetime should be drawn (see appendix D). Each diagonal line on such a diagram represents a light cone. The two inequivalent null slicings can hence be represented by the ascending and descending families of diagonal lines. The apparent horizon will divide the spacetime into normal, trapped and anti-trapped regions. Hence, after choosing one family, each diagonal line should be projected in the direction of positive expansion and onto the nearest point where the expansion changes sign or where the spacetime ends. The end points (surfaces) will then form the screen-hyersurface(s) of the spacetime.

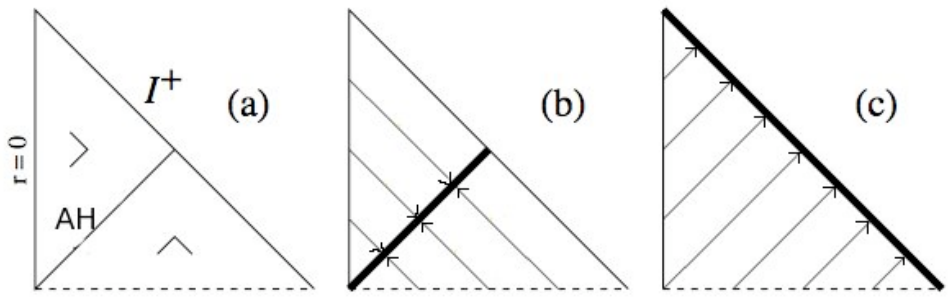

Figure 3.1: A Penrose diagram for a flat radiation-filled FRW space (a). The information contained in the entire spacetime can be projected on the apparent horizon (b) or onto the null infinity (c)

Part II

Saturating the Covariant Bound

Chapter 4

Saturation in FRW cosmology

In the previous chapters we found a universally valid bound on the entropy amount that a spacetime region can posses. The entropy of matter on a light sheet L orthogonal to a spatial surface B cannot exceed the surface area A, measured in Planck units:

$$S\left[L(B)\right] \leq \frac{A(B)}{4} \tag{4.1}$$

We have found that black holes exactly saturate this bound. For ordinary matter systems however, not carrying any Bekenstein-Hawking entropy, it seems difficult to saturate the bound (4.1). Furthermore, a stronger bound seems to be valid in this case: many examples suggest matter systems obey

$$S \leq A^{3/4}. \tag{4.2}$$

4.1 Flat FRW universe

As an illustration that the bound (4.2) might hold for ordinary matter, we consider a flat Friedmann-Robertson-Walker (FRW) universe. Suppose it is filled with radiation and with a cosmological constant $\Lambda = 0$. The cross-sectional area of the past light-cone of an observer will initially expand, but consequently contract until it vanishes at the Big Bang. Thus, there will exist a sphere of maximum area, A_{AH}. Let's assume the observer at a time t_E and comoving radius $\xi = 0$. The metric of such a universe is

$$ds^2 = -dt^2 + a(t)^2 \left(d\xi^2 + \xi^2 d\Omega^2\right) \tag{4.3}$$

The following relations will be valid for light rays:

$$\begin{aligned} &\frac{dt}{a} = d\xi && \text{(light rays)} \\ &p = \frac{1}{3}\rho && \text{(equation of state)} \\ &H^2 = \rho/3 && \text{(Friedmann)} \\ &\dot{\rho} + 4H\rho = 0 && \text{(conservation of energy)} \end{aligned} \tag{4.4}$$

From these equations one can easily find that $\rho \propto a^{-4}$ and $a \propto t^{1/2}$.
The past light cone of the observer will obey

$$\begin{aligned} & 2\Delta t^{1/2} = \Delta\xi \\ \Rightarrow \quad & \xi/2 = t_E^{1/2} - t^{1/2} \end{aligned} \tag{4.5}$$

The apparent horizon satisfies (we will later show that $A_{AH} \propto \rho^{-1}$)

$$t^{1/2} = \xi/2 \tag{4.6}$$

Combining equations (4.5) and (4.6), we find the relation $t_E = 4t$ between the time of the observer t_E and the time t when the past light sheet intersects the apparent horizon. Hence, the area of the apparent horizon will be proportional to t_E^2:

$$\begin{aligned} A_{AH} &\propto a^2\xi^2 \\ &\propto t \cdot t \\ &\propto t_E^2 \end{aligned} \tag{4.7}$$

The sphere of maximum area A_{AH} will thus be the origin of two light-sheets: one future-directed and one past-directed. We find that the comoving size of the past light-cone is of the order of the region inside the Hubble horizon at time t_E: setting $t = 0$ in equation (4.5), we find $\xi = 2t_E^{1/2}$, and the same result is found from $V_{hor} \propto t^3 \sim a^3\xi^3$. If we assume an adiabatic evolution, the entropy contained in the light-cone will be the same as the entropy inside the Hubble horizon at time t_E. From the equations (4.4), we find a proper energy density $\rho_{rad} \sim t_E^2$. If we consequently assume the entropy density of the radiation is related to the energy density as $s \sim \rho_{rad}^{3/4} \sim t_E^{-3/2}$, the total entropy on the light-sheets will be

$$S \sim t_E^{-3/2} V_{hor} \sim t_E^{3/2} \sim A_{AH}^{3/4}, \tag{4.8}$$

We thus find that equation (4.2) is approximately saturated.

However, in contrast with this example, most of the ordinary matter systems will not even come close to saturating equation (4.2) (see for example [2]), hence the the holographic bound (4.1) might seem needlessly weak and a stronger bound might be more fundamental. In the next sections will be shown that the bound (4.2) can indeed be exceeded, confirming the universality of the holographic bound. The cosmological examples in the next sections will always assume an average energy density and entropy density throughout the universe. In the case of radiation domination, they will be related by $s \sim \rho_{rad}^{3/4}$, and in the case of matter domination by $s \sim \rho/m$. By the FMW theorems, the holographic bound (4.1) will always be valid in these universes. We will indeed focus on finding examples exceeding the bound (4.2) and not trying to find counterexamples for holographic bound. Furthermore, we will assume adiabatic evolution, implying that the entropy density is related to the constant comoving entropy density σ: $s = \sigma/a^3$

4.2 Truncated Light-Sheets

In this section we will find a special class of light-sheets, on which the entropy will exceed the bound $S \leq A^{3/4}$. Again, let's consider a flat, radiation dominated FRW universe, as in the previous section. At a fixed time t_0, spheres with a very large radius ξ_0 will be anti-trapped and thus have two past-directed light-sheets. The ingoing light-sheet obeys

$$\begin{aligned} & 2\Delta t^{1/2} = \Delta\xi \\ \Rightarrow \quad & 2(t_0^{1/2} - t^{1/2}) = \xi_0 - \xi \end{aligned} \tag{4.9}$$

If we demand that ξ_0 is larger than the particle horizon at time t_0, the light sheet will be truncated at the big bang. In this case, we can assume that the final comoving radius, at the big bang, will still be very large. Setting $t = 0$ in equation (4.9) we find $\xi = \xi_0 - 2t_0^{1/2}$, and a very large comoving radius implies $\xi_0 \gg t_0$. The entropy on the light-sheets is $S = \sigma V_c$, where $V_c \sim (\xi_0^3 - \xi^3)$ is the comoving volume of the light-sheets. In our case we find

$$\begin{aligned} V_c &\sim \xi_0^3 - \xi^3 \\ &\sim \left(\xi_0^3 - (\xi_0 - 2t_0^{1/2})^3\right) \\ &\sim \left(\xi_0^3 - \xi_0^3(1 - 2\frac{t_0^{1/2}}{\xi_0})^3\right) \\ &\sim \left(\xi_0^3 - \xi_0^3(1 - 6\frac{t_0^{1/2}}{\xi_0})\right) \\ &\sim \xi_0^2\ t_0^{1/2} \end{aligned} \tag{4.10}$$

A similar calculation for the outgoing light-sheet would lead to exactly the same result. The surface area is $A \sim a_0^2\ \xi_0^2 \sim t_0\ \xi_0^2$, hence we finally retrieve

$$S/A \sim t_0^{-1/2} \tag{4.11}$$

In the derivation of the last equation, we assumed the comoving entropy density $\sigma \sim 1$. This corresponds to the assumption that at the planck time $t_p = 1$, the entropy in every planck volume is equal to its surface area:

$$(S/A)_{t_p} \sim \sigma\ \frac{\xi_p}{a_p^2} \sim \sigma \tag{4.12}$$

From equation (4.10), one finds that $S > A^{3/4}$ if $A^{1/4} \gg t_0^{3/2}$, which is the case when $\xi_0 \gg t_0^{5/2}$. Intuitively one can understand this the following way: the truncated light-sheets have constant comoving width, and, for a fixed time, the comoving volume is proportional to A when increasing the radius. Hence also the entropy $S \sim V_c$ is proportional to A , and the bound (4.2) will be violated as soon the radius is large enough.

This class of light-sheets can be found as well in open and closed FRW universes. However, the drawback of these surfaces is that we require a radius far beyond the particle horizon. In the next section we will show some examples where this is not the case. Let's first of all remark that the right hand side of equation (4.10) is independent of the surface area A, which allows us to find a violation of $S \geq A^{3/4}$. We would like to find counterexamples that are related to the one above. In general, the entropy-area ratio is $S/A = \sigma V_c/A$. Hence, in order for the right hand side to be independent of the area, the term V_c/A should be independent of A (but not vanishing). Lets review this term for different FRW universes, assuming that the light sheet reaches $\xi = 0$:

$$\begin{aligned}
&\text{Flat FRW:} && \text{Closed FRW:} \\
&V_c = \int \xi^2 d\xi d\Omega^2 = \frac{4\pi}{3}\xi^3 && V_c = \int \sin^2\xi d\xi d\Omega^2 = \pi\left[2\xi - \sin(2\xi)\right] \\
&A_c = \int \xi^2 d\Omega^2 = 4\pi\ \xi^2 && A_c = \int \sin^2\xi d\Omega^2 = 4\pi\ \sin^2\xi \\
\Rightarrow\quad &\frac{V_c}{A_c} \propto \xi && \Rightarrow\quad \frac{V_c}{A_c} \propto \frac{2\xi - \sin(2\xi)}{\sin^2\xi}
\end{aligned} \tag{4.13}$$

$$\begin{aligned}
&\text{Open FRW:} \\
&V_c = \int \sinh^2\xi d\xi d\Omega^2 = \pi\left[\sinh(2\xi) - 2\xi\right] \\
&A_c = \int \sinh^2\xi d\Omega^2 = 4\pi\ \sinh^2\xi \\
\Rightarrow\quad &\frac{V_c}{A_c} \propto \frac{\sinh(2\xi) - 2\xi}{\sinh^2\xi}
\end{aligned} \tag{4.14}$$

It is clear from equations (4.13) that the right hand side remains proportional to $\xi \sim A_c^{1/2}$, thus making it impossible imposing $A^{1/4}$ much bigger then the right hand side. In the case of the open universe, however, one finds a special feature. Choosing a comoving radius sufficiently larger than 1, one can approximate $\sinh\xi \sim \exp\xi$. Hence the dependance on ξ will dissapear:

$$\frac{V_c}{A_c} \sim \frac{\exp(2\xi)}{\exp(2\xi)} \tag{4.15}$$

In the next section, we will therefore review a class of counterexamples that exist only in open universes, for which the comoving radius need not to be larger then the particle horizon.

4.3 Open FRW Universes

An important surface will be the one where the expansion of the light-rays vanishes, which is called the apparent horizon. We will derive a general expression for this surface first. The

expansion (see section (3.2.2)) is given by

$$\theta = \frac{dA/d\lambda}{A} \tag{4.16}$$

Using $A \propto a^2 f^2$ and $\lambda = \pm 2t, \lambda = \pm 2\xi$ (where $f = \xi, \sin\xi, \sinh\xi$ for flat, closed and open universes respectively) one finds:

$$\theta_{+\pm} = \frac{\dot{a}}{a} \pm \frac{f'}{f}, \quad \theta_{-\pm} = -\frac{\dot{a}}{a} \pm \frac{f'}{f} \tag{4.17}$$

A dot (prime) stands for the derivation with respect to t (ξ). The apparent horizon has vanishing expansion, hence

$$\frac{\dot{a}}{a} = \pm\frac{f'}{f} \tag{4.18}$$

Using $f' = \sqrt{1 - kf^2}$ we find $f_{AH}^2 = \left((\frac{\dot{a}}{a})^2 + k\right)^{-1}$, where $k = 0, -1, +1$ for flat, closed and open universes respectively. Eventually, the apparent horizon is given by

$$A_{AH} = 4\pi a^2 f_{AH}^2 = \frac{4\pi^2}{(\frac{\dot{a}}{a})^2 + k} = \frac{3}{2\rho}, \tag{4.19}$$

In the last step of equation (4.19), we used the Friedmann equation,

$$\frac{\dot{a}^2}{a^2} = \frac{8\pi\rho}{3} - \frac{k}{a^2} \tag{4.20}$$

The metric of an open FRW universe is given by

$$ds^2 = -dt^2 + a(t)\left[d\xi^2 + \sinh^2\xi d\Omega^2\right] \tag{4.21}$$

The terms inside the square bracket form the metric on the unit three-hyperboloid. The comoving area and volume of a sphere of radius ξ are given by equations (4.14).
Let's first consider a radiation-dominated open FRW universe. The energy density will then contain a radiation component and a vacuum energy component, $\rho = \rho_r + \rho_\Lambda$. The cosmological constant is $\Lambda = 8\pi\rho_\Lambda$, hence the Friedmann equation can be written as

$$\dot{a}^2 a^2 = t_c^2 + a^2 \pm \frac{a^4}{t_\Lambda^2}, \tag{4.22}$$

where $t_c = \left[\left(8\pi\rho_r\ a^4\right)/3\right]^{1/2}$ characterizes when the curvature term becomes dominant, and $t_\Lambda = |3/\Lambda|^{1/2}$ determines when the vacuum term becomes dominant. The class of light-sheets we will consider, originate in the curvature era. We will thus assume

$$t_c \ll t_\Lambda \tag{4.23}$$

During this era, the scale factor is approximately equal to the time,

$$\frac{\dot{a}^2}{a^2} \propto a^{-2} \quad \Rightarrow \quad da \propto dt, \tag{4.24}$$

hence it will be often convenient to use the scale factor a instead of the time coordinate t. Moreover, we will continue doing this for the other eras, when the time and scale factor are not in agreement anymore.

Consider now a two dimensional sphere during the curvature era. Let's call the comoving radius of the sphere ξ_0 and suppose the scale factor equal to $a_0 \gg t_c$. The proper area of the sphere will be

$$A = 4\pi a_0^2 \sinh^2 \xi_0 \tag{4.25}$$

We will assume that the sphere lies outside the apparent horizon, so we can construct the past outgoing light-sheet. From equation (4.21), we find that this light-sheet obeys

$$\xi(t) = \xi_0 + \int_t^{t_0} \frac{d\bar{t}}{a(\bar{t})} = \xi_0 + \int_t^{t_0} \frac{d\bar{a}}{\bar{a}\dot{\bar{a}}} \tag{4.26}$$

We can now insert equation (4.22),

$$\xi(t) = \xi_0 + \int_t^{t_0} \frac{d\bar{a}}{\sqrt{t_c^2 + a^2 \pm a^4/t_\Lambda^2}} \tag{4.27}$$

Let's call a_1 the time where the light-sheet ends, at the corresponding radius $\xi_1 = \xi(a_1)$. The entropy on the light-sheet can be calculated using

$$S = \sigma V_L \tag{4.28}$$

where $V_L = V_c(\xi_1) - V_c(\xi_0)$ is the comoving volume of the light-sheet and the comoving entropy density is $\sigma = \rho_r^{3/4} a^3 \sim t_c^{3/2}$. Here we have used the same relation between the entropy density and the radiation energy density as before, $s \sim \rho_r^{3/4}$. We will now calculate equation (4.28) for a zero, negative and positive cosmological constant.

4.3.1 Zero Cosmological Constant

For a vanishing cosmological constant, the last term under the square root in equation (4.27) is zero, and hence the equation can be integrated, using $\int (a^2 + x^2)^{-1/2} dx = \sinh^{-1}(x/a)$, giving the following result for the light-sheet:

$$\xi(a) = \xi_0 + \sinh^{-1}(a_0/t_c) - \sinh^{-1}(a/t_c) \tag{4.29}$$

From $a_0^2 \sinh^2 \xi_0 \sim A \geq A_{AH} \sim a_0^4/t_c^2$ we find $\sinh^2 \xi_0 \geq a_0^2/t_c^2 \gg 1$, since $a_0 \gg t_c$. The light-sheet under consideration is an outgoing light-sheet, hence we have $\xi_1 > \xi_0 \gg 1$. We can therefore approximate the comoving volume $V_c \approx \pi/2 \exp(2\xi)$. Let's now calculate the entropy for $t_c \ll a_1 \ll a_0$. For this purpose, we will use the taylor expansion of $\sinh^{-1}$,

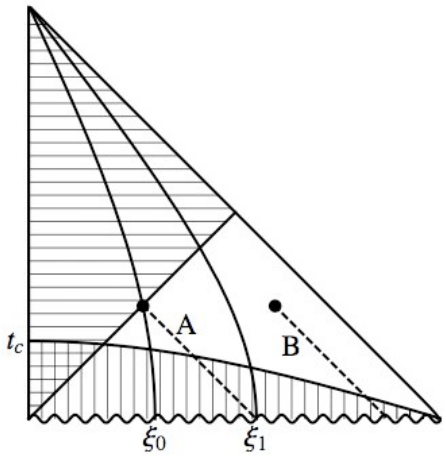

Figure 4.1: The conformal diagram of an open, radiation filled FRW universe with zero cosmological constant. Two light-sheets are shown, one that starts on the apparent horizon (A), and one that starts well outside (B). (This image was copied from [2])

$$\sinh^{-1} = \begin{cases} x - \frac{x^3}{2\cdot 3} + \frac{1\cdot 3x^5}{2\cdot 4\cdot 5} - \frac{1\cdot 3\cdot 5x^7}{2\cdot 4\cdot 6\cdot 7} + ... & (|x| < 1) \\ \pm\left(\ln|2x| + \frac{1}{2\cdot 2x^2} - \frac{1\cdot 3}{2\cdot 4\cdot 4x^4} + ...\right) & (\ +\text{ if } x \geq 1;\ -\text{ if } x \leq -1) \end{cases} \tag{4.30}$$

The entropy then is

$$\begin{aligned} S &\sim \sigma V_L \\ &\sim t_c^{3/2} \exp(2\xi_1) \\ &\sim t_c^{3/2} a_0^2 \exp(2\xi_0) \cdot \frac{1}{a_0^2} \exp^2(\xi_1 - \xi_0) \\ &\sim t_c^{3/2}\ A\ a_1^{-2} \end{aligned} \tag{4.31}$$

where we made use of

$$\begin{aligned} \exp(\xi_1 - \xi_0) &= \exp\left(\sinh^{-1}(a_0/t_c) - \sinh^{-1}(a_1/t_c)\right) \\ &= \frac{\exp\left(\sinh^{-1}(a_0/t_c)\right)}{\exp\left(\sinh^{-1}(a_1/t_c)\right)} \\ &\sim \frac{\exp\left(\ln 2(a_0/t_c)\right)}{\exp\left(\ln 2(a_1/t_c)\right)} \\ &\sim \frac{a_0}{a_1} \end{aligned} \tag{4.32}$$

It is clear from equation (4.31) that the light-sheet will contain more entropy the longer it is (the smaller a_1 is). Since we are interested in maximizing the entropy, let's extend the light-sheet to $a_1 \to 0$. We are then in the regime $a_1 \ll t_c \ll a_0$, and making derivation

similar to equations (4.31) and (4.32) we find for the entropy on the light-sheet:

$$\begin{aligned} S &\sim \sigma V_L \\ &\sim t_c^{3/2}\ A\ \left[\frac{\exp(\xi_1-\xi_0)}{a_0}\right]^2 \\ &\sim t_c^{3/2}\ A\ \left[\frac{\exp(\ln 2(a_0/t_c))}{a_0\ \exp(a_1/t_c)}\right]^2 \\ &\sim t_c^{3/2}\ A\ \frac{1}{t_c^2}\frac{1}{(1+a_1/t_c)^2} \\ &\sim \frac{A}{t_c^{1/2}}\left(1-2\frac{a_1}{t_c}\right) \end{aligned} \tag{4.33}$$

Extending the light-sheet to the big bang ($a_1 \to 0$ in equation (4.33)) does not add significant entropy to the light-sheet when we end it at t_c ($a_1 \to t_c$ in equation (4.31)). Up to factors of order one, the entropy/area ratio will be

$$\frac{S}{A} \sim t_c^{-1/2} \tag{4.34}$$

Using $t_c \geq 1$ and $A^{1/4} \geq 1/t_c^{1/2}$, it follows that $A^{3/4} \ll S \leq A$. The entropy will thus violate equation (4.2) in this example. Choosing $t_c \sim 1$, i.e. a very early curvature domination of the order of the Planck time, one can saturate the holographic bound. We remark that in this case, the final edge of the light-sheet will be near the Planck regime.

Pressureless Matter

The same results can be obtained in an open universe filled with pressurless dust, instead of radiation. The first difference will concern the energy density of the pressureless dust, which is given by

$$\frac{8\pi\rho}{3} = \frac{t_c}{a^3}, \tag{4.35}$$

which results in the following Friedmann equation,

$$a^2\dot{a}^2 = t_c a + a^2. \tag{4.36}$$

We will again choose a sphere well inside the curvature era, $t_c \ll a_0 \ll t_\Lambda$, and who's area exceeds the apparent horizon, $\xi_0 > \xi_{AH} \approx \frac{1}{2}\ln(\frac{a_0}{t_c})$. This last equation can be deduced by using $A_{AH} = \frac{3}{2\rho} \sim \frac{a_0^3}{t_c}$ and $A_{AH} \sim a_0^2 \exp(2\xi_{AH})$. The past outgoing light-sheet is then given by

$$\begin{aligned} \xi(a) &= \xi_0 + \int_a^{a_0} \frac{d\bar{a}}{\sqrt{t_c\bar{a}+\bar{a}^2}} \\ &= \xi_0 + 2\sinh^{-1}\left(\sqrt{a_0/t_c}\right) - E\sinh^{-1}\left(\sqrt{a/t_c}\right), \end{aligned} \tag{4.37}$$

where we made use of

$$\int \frac{dx}{\sqrt{ax+x^2}} = 2a \int \frac{\sqrt{\frac{x}{a}} d\sqrt{\frac{x}{a}}}{\sqrt{ax}\sqrt{1+x/a}} = 2\sinh^{-1}\sqrt{x/a}. \tag{4.38}$$

Furthermore, the entropy density of the pressureless dust is of the order of the number density of the particles,

$$s \sim \frac{\rho}{m} \sim \frac{t_c}{ma^3}. \tag{4.39}$$

The same argument concerning a_1 applies in this case: the dominant contribution will be come from the curvature dominated era, and hence we will set $a_1 = t_c$ as before. The comoving volume contained by the light-sheet will be

$$\begin{aligned} V_L &\sim e^{2\xi_1} \sim\sim e^{2\xi_0} \sim e^{2(\xi_1-\xi_0)} \\ &\sim e^{2\xi_0} \frac{\exp^4(\ln\left|2\sqrt{a_0/t_c}\right|)}{\exp \mathcal{O}(1)} \\ &\sim e^{2\xi_0} \frac{a_0^2}{t_c^2} \end{aligned} \tag{4.40}$$

We finally find, using $A \sim a_0^2 e^{2\xi_0}$,

$$S/A = \frac{t_c}{m}\frac{V_L}{A} = (mt_c)^{-1} \tag{4.41}$$

If we choose the radius large enough, satisfying $1 < mt_c < A^{1/4}$, the entropy will again exceed the naive $S \leq A^{3/4}$. For $mt_c \to 1$, the holographic entropy bound will be saturated. The case $mt_c \ll 1$ is impossible, since equation (4.39) is only valid if the particles are dilute. This translates in the requirement that the density of the particles is less than one particle per Compton wavelength cubed,

$$\begin{aligned} &\lambda_{Compt} = \frac{h}{mc} \\ &\rho/m < \lambda_{Compt}^{-3} = m^3 \quad \Rightarrow \quad t_c^{-2}/a^3 < m^4 \end{aligned} \tag{4.42}$$

If we want last equation to be valid for all a in the considered era $a_1 \leq a \leq a_0$, it follows that

$$t_c^{-1/2} < m \tag{4.43}$$

The assumption of an entropy density as in equation (4.39) thus allows a saturation of the holographic bound, but it can never be violated (cfr. FMW).

4.3.2 Positive Cosmological Constant

In the case of an open universe with positive cosmological constant, the apparent horizon will be

$$A_{AH}(t) = \frac{3}{2\left(\rho_\Lambda + \rho_r\right)} = 4\pi\left(\frac{t_c^2}{a^4} + \frac{1}{t_\Lambda^2}\right)^{-1} \tag{4.44}$$

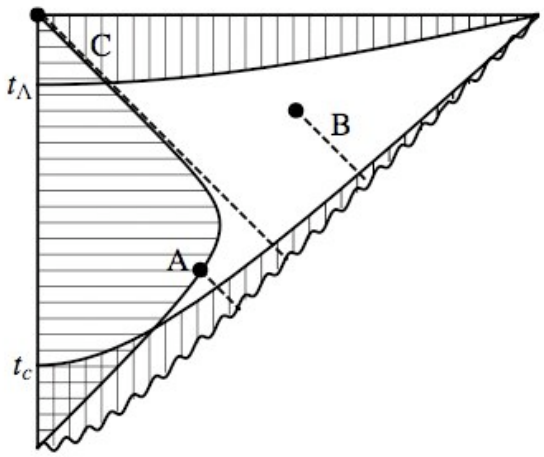

Figure 4.2: The conformal diagram of an open, radiation filled FRW universe with positive cosmological constant. Three light-sheets are shown, one that starts on the apparent horizon (A), one that starts well outside (B) and one that coincides with the de Sitter event horizon (C). This image was copied from [2]

From this equation one can easily find that the apparent horizon asymptotes to $A_{dS} = \frac{12\pi}{\Lambda} \sim t_\Lambda^2$, the event horizon of de Sitter space, for $t \gg t_\Lambda$. As the previous case, we will consider spheres with area greater than the apparent horizon, so that a past-directed outgoing light-sheet exists.

First, consider $t_c \ll a_0 \leq t_\Lambda$. In this case the a^4/t_Λ^2 term in equation (4.27) can be neglected, which brings us to exactly the same analysis as in a universe with zero cosmological constant. We can thus make exactly the same conclusion as the previous section.

For $a_0 \gg t_\Lambda$, we find from equation (4.27),

$$\begin{aligned}\xi_1 - \xi_0 &\sim \int_{t_\Lambda}^{a_0} \frac{t_\Lambda d\bar{a}}{\bar{a}^2} + \int_{t_c}^{t_\Lambda} \frac{d\bar{a}}{\bar{a}} \\ &\sim t_\Lambda \left(\frac{1}{t_\Lambda} - \frac{1}{a_0}\right) + \ln \frac{t_\Lambda}{t_c} \\ &\sim \ln \frac{t_\Lambda}{t_c} \qquad (a_0 \gg t_\Lambda \gg t_c)\end{aligned} \tag{4.45}$$

We used $a_1 \sim t_c$ like in the previous section, in order to maximize the entropy, which can is equal to

$$\begin{aligned}S &\sim t_c^{3/2} e^{2\xi_0} e^{\xi_1 - \xi_0} \\ &\sim e^{2\xi_0} \frac{t_\Lambda^2}{t_c^{1/2}}\end{aligned} \tag{4.46}$$

For $\xi_0 \geq 1$, the proper area of the surface is given by $A \sim a_0^2 e^{2\xi_0}$, resulting in $S/A \sim t_c^{-1/2} (t_\Lambda/a_0)^2$, which is much smaller than $t_c^{-1/2}$. Hence, this case does not result useful. For

$\xi_0 \ll 1$, on the other hand, one obtains $S/A \sim t_c^{-1/2}\,(A_{dS}/A)$, where we used $A_{dS} \sim t_\Lambda^2$. Since the surface is assumed bigger than the apparent horizon, and since $\exp\xi_0 \ll 1$ one finds $A_{dS} \leq A \ll a_0^2$. An initial area close to the de Sitter event horizon will result in

$$S/A \sim t_c^{-1/2}. \tag{4.47}$$

A special case will arise when taking $a_0 \to \infty, \xi_0 \to 0, A = A_{dS}$. The light-sheet will then correspond to the de Sitter event horizon, which can be seen to saturate the holographic bound if the curvature era begins very early, $t_c \to A$.

Pressureless Matter

This case can readily be applied to a universe filled with pressureless dust. The Friedmann equation is

$$a^2\dot{a}^2 = t_c a + a^2 + \frac{a^4}{t_\Lambda^2}. \tag{4.48}$$

Both the $t_c \ll t_0 \leq t_\Lambda$ and the $t_\Lambda \ll t_0$ case are completely analogous to the radiation dominated universe, and hence the same results are obtained.

4.3.3 Negative Cosmological Constant

For a radiation-filled universe with negative cosmological constant, the apparent horizon is

$$A_{AH}(t) = \frac{3}{2\left(\rho_\Lambda + \rho_r\right)} = 4\pi\left(\frac{t_c^2}{a^4} - \frac{1}{t_\Lambda^2}\right)^{-1} \tag{4.49}$$

The negative vacuum energy implies that at a time $t_* = (t_c t_\Lambda)$, the total energy density will vanish and then become negative, as follows from

$$\rho_{tot} = 0 \Rightarrow \frac{8\pi\rho_\Lambda}{3} = \frac{8\pi\rho_r}{3} \Rightarrow t_c^2 t_\Lambda^2 = a^4 \tag{4.50}$$

The apparent horizon becomes infinite for $t \to t_*$, and does not exist at any later times. Hence, the past-directed outgoing light sheets will only exist for times smaller then t_*. We will therefore require $a_0 < t_*$, and since $t_* \ll t_\Lambda$, the last term in equation (4.27) can again be neglected. The analysis will be identical to the $\Lambda = 0$ case, where the entropy exceeds $A^{3/4}$, and approximately saturates the holographic bound for $t_c \to 1$.

However, an additional class of light-sheets can be found who's entropy exceeds $A^{3/4}$. The spheres under consideration will be normal. Consider $t_* \leq t_0 \leq t_f - t_*$. During this era, all spheres are normal since there is no apparent horizon. We will look at the past directed ingoing light-sheet (the future-directed case is analogous). Suppose we terminate the light-sheet at the time t_*, then it follows from

$$\Delta\xi = \xi_0 - \xi_* \sim \int_{t_*}^{t_0} \frac{da}{a} \sim \ln\frac{t_0}{t_*} \tag{4.51}$$

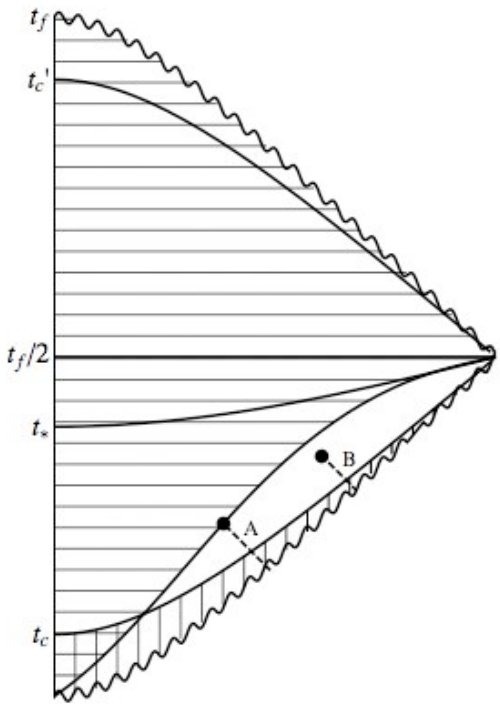

Figure 4.3: The conformal diagram of an open, radiation filled FRW universe with negative cosmological constant. Two light-sheets are shown, one that starts on the apparent horizon (A), and one that starts well outside (B). This image was copied from [2]

that $\Delta\xi$ will exceed unity if t_0 is at least a few times larger than t_*. In this case the comoving volume can be approximated by $V_L \approx V_c(\xi_0)$, and the entropy on the light sheet $S \sim e^{2\xi_0} t_c^{3/2}$. The initial area is $A \sim a_0^2 e^{2\xi_0}$, hence

$$S/A \sim \frac{t_c^{3/2}}{t_0^2} \tag{4.52}$$

This ratio can be maximized for $t_0 \to t_*$, obtaining $S/A \sim t_c^{-1/2} \frac{t_c}{t_\Lambda}$. Due to $t_c \ll t_\Lambda$, this is a lot smaller than the ratio $t_c^{-1/2}$ in the anti-trapped case. The holographic bound cannot be saturated, however the light-sheets do violate the naive $S \leq A^{3/4}$ if we choose the initial radius large enough (choosing $t_c^{3/2}/t_0^2 \gg A^{-1/4} \sim a_0^{-1/2} e^{-\xi_0/2}$).

This class of light-sheets can also be found in flat universes with negative cosmological constant. In the flat case, the turnaround time $t_f/2$ (for which $\dot{a} = 0$) is given by

$$0 = t_c^2 - \frac{a^4}{t_\Lambda^2} \Rightarrow t_f/2 = t_*. \tag{4.53}$$

The apparent horizon will now only diverge at this point in time, and hence for very large comoving radius, normal spheres will exist only for a very short time around $t_f/2$. Consider

$t_0 = t_f/2$, and suppose we terminate the light-sheet at an early time $t_1 = t_\Lambda^2/t_c \ll t_\Lambda < t_c$. We find

$$\begin{aligned}\Delta\xi &= \int_{t_1}^{t_*} \frac{da}{\sqrt{t_c^2 - a^4/t_\Lambda^2}} \\ &\sim \int_{t_1}^{t_*} \frac{da}{t_c} \quad (\text{for } t_1 < a < t_* : t_c^2 > a^4/t_\Lambda^2) \\ &\sim t_*/t_c = (t_\Lambda/t_c)^{1/2} \end{aligned} \tag{4.54}$$

Hence, $\Delta\xi \ll 1$, and we can treat the comoving light-sheet as a thin shell. We finally find $S \sim t_c^{3/2}\xi_0^2\Delta\xi$ and $A \sim t_*^2\xi_0^2$, which leads to the ratio

$$S/A \sim t_\Lambda^{-1/2} \tag{4.55}$$

The light-sheet is found to violate the $S \leq A^{3/4}$ for a sufficiently large radius which satisfies $t_\Lambda^{-1/2} \gg A^{-1/4}$. Let's remark, however, that we were forced to extend the light-sheet into the anti-trapped region.
Just as for the universes with positive and zero cosmological constant, the case for negative cosmological constant can straightforwardly be adapted for a universe filled with pressureless dust.

4.4 Observable Entropy

In this section we will show that some of the light-sheets previously considered exist in the past of an event. Hence the light-sheet itself and the entropy contained on it will be observable.

We consider, like in the previous section, open universes with zero, negative and positive cosmological constant and a curvature era that satisfies $t_c \ll t_\Lambda$. Since we the FRW universe is homogeneous, we consider the observer at the origin, $\xi = 0$. Let's call $L(t_E)$ the past light-cone of an event at t_E and $\xi = 0$, then the disjoint union of all these light-cones is called the causal patch of the observer. Hence, the causal patch will be the region of the spacetime that can be observed.

4.4.1 Finite time

First of all, let's look at the entropy on one such a light-sheet. Hence, we consider the observer at finite time t_E. The cross-sectional area of its past light-cone will vanish at t_E, but also at the big bang. Thus, there will exist a sphere of maximum area in between, the apparent horizon. The time t_0 at which we find the apparent horizon is a monotonically growing function of the observer time t_E, as can be shown in a similar way like equations (4.5) and (4.6).

The apparent horizon divides the light cone $L(t_E)$ in two pieces, L_{in} which covers $t_0 \leq t \leq t_E$ and L_{out} which covers $t_0 \geq t > 0$. The cross-sectional area of both pieces will be decreasing when followed away from the apparent horizon, hence both will be light-sheets of the sphere at t_0. The outgoing light-sheet is precisely one like we considered in the previous section. We will now see that it can indeed contain large entropy. We have showed in section (4.3) that the outgoing light-sheet will satisfy $S/A \sim t_c^{-1/2}$ if the initial surface is well inside the curvature era, $t_0 \gg t_c$. Suppose that indeed $t_0 \gg t_c$, and suppose $\Lambda = 0$. We find

$$\xi_{AH}(t_0) = 0 + \int_{t_0}^{t_E} \frac{da}{a} = \ln \frac{t_E}{t_0} \tag{4.56}$$

The area of the apparent horizon sattisfies $A_{AH} \sim a_0^2 \exp^2(\xi_{AH}(t_0)) \sim a_0^4/t_c^2$, resulting in $\xi_{AH}(t_0) \sim \ln t_0/t_c$. Using equation (4.56) we find

$$\ln t_0/t_c = \ln t_E/t_0 \Rightarrow t_0^2/t_c \sim t_E. \tag{4.57}$$

Hence, the conditions $t_E \gg t_c$ and $t_0 \gg t_c$ are equivalent. We have thus found that the past light-cone of an observer at t_E can indeed contain very large entropy, provided that $t_E \gg t_c$.

This result is also valid for $\Lambda \neq 0$, even if t_E lies in the vacuum dominated era $t_E \geq t_\Lambda$. Indeed, t_0 is a monotonic function of t_E and hence will grow even bigger. As we showed in previous sections, past-directed outgoing light-sheets of this kind (for the case $\Lambda < 0$ with $t_0 \gg t_c$ and for the case $\Lambda > 0$ with $t_0 \gg t_c$ and $A \leq A_{\text{dS}}$) will always satisfy $S/A \sim t_c^{-1/2}$. The case above equation (4.47) cannot hold for the past light-cone of an observer, because the past-directed light-sheet starts from the apparent horizon, and from equation (4.44) it is clear that the condition $A_{AH} > A_{dS}$ is never satisfied in this case.

The entropy contribution of the inner light-sheet will be negligible compared to that of the outer light-sheet, since the entropy on the inner one will not exceed $S \sim A^{3/4}$. Hence, for all $t_E \gg t_c$, the entropy in the past light-cone of an observer will be

$$S(L) \sim A_{AH} t_c^{-1/2}, \tag{4.58}$$

where A_{AH} is the maximum area of the past light-cone, which obeys

$$A_{AH} \sim \left(1/a_E^4 \pm 1/t_\Lambda^2\right) \sim \left(1/t_E^2 \pm 1/t_\Lambda^2\right). \tag{4.59}$$

Because the lowest value we can find for $A_{AH}^{1/4}$ is (approximately) equal to $t_E^{1/2}$ for $\Lambda \leq 0$ and to $\min\left(t_E^{1/2}, t_\Lambda^{1/2}\right)$ for $\Lambda > 0$, it is clear that the entropy will exceed $A_{AH}^{3/4}$ by this large amount:

$$\begin{aligned} S &\sim A_{AH} t_c^{-1/2} \\ &\sim A_{AH}^{3/4}\ A_{AH}^{1/4}\ t_c^{-1/2} \\ &\geq A_{AH}^{3/4} \end{aligned} \tag{4.60}$$

4.4.2 The Causal Patch

Now let's consider the entropy in the whole causal patch, by taking $t_E \to \infty$. From equations (4.59) and (4.60) it is clear that, in the $\Lambda = 0$ case, the entropy is unbounded. We will now look at the two remaining cases $\Lambda < 0$ and $\Lambda > 0$.

Positive Cosmological Constant

In the $\Lambda > 0$ case, the past light-cone becomes the de Sitter event horizon when taking the limit $t_E \to \infty$. Its area is decreasing everywhere towards the big bang, hence the whole horizon is one light-sheet. Moreover, all the observable radiation will pass through this horizon, and hence the entropy contained on the light-sheet will be the maximum possible observable entropy, S_{max}. The same light-sheet was obtained, albeit using another limit, under equation (4.47). The entropy on it will therefore be equal to

$$S_{max} \sim A_{dS} t_c^{-1/2} \sim \Lambda^{-1} t_c^{-1/2} \tag{4.61}$$

For $t_\Lambda \gg t_c$ we have $\Lambda^{-1/4} \gg t_c^{-1/2}$ and the bound $S_{max} < \Lambda^{-3/4}$, which holds for a flat radiation dominated FRW universe, is exceeded. For early curvature domination, the entropy will be $S_{max} \to \Lambda^{-1}$.

Negative Cosmological Constant

In the case of a negative cosmological constant, the light-cone of an event at $t_E \to \infty$ will reach $\xi_{max} = 2\xi_{turn}$, because the evolution is symmetric about the time of maximal expansion t_{turn}. We can calculate this coordinate,

$$\xi_{turn} \sim \int_0^{a_{max}} \frac{d\bar{a}}{\sqrt{t_c^2 + \bar{a}^2 + \bar{a}^4/t_\Lambda^2}} \sim \int_{t_c}^{a_{max}} \frac{d\bar{a}}{\bar{a}} \sim \ln \frac{t_\Lambda}{t_c} \tag{4.62}$$

The entropy inside a sphere with comoving radius ξ is $S(\xi) = \sigma V_c(\xi)$, and like before we will use $\sigma \sim t_c^{3/2}$. The comoving volume for the case $t_E \to \infty$ can be approximated as $V_c \sim \exp(2\xi_{max}) \sim e^{4\xi_{turn}}$. Hence the entropy in the causal patch will be

$$S_{max} \sim \frac{t_\Lambda^4}{t_c^{5/2}} \sim \Lambda^{-2} t_c^{-5/2} \tag{4.63}$$

Again, this shows that the observable entropy violates the naive $S < |\Lambda|^{-3/4}$ and that it approaches $S_{max} \to \Lambda^{-2}$ in the limit of early curvature domination.

Let's note that the time t_0, where the causal patch intersects the apparent horizon, obeys $t_c \ll t_0 \ll t_\Lambda$. The first inequality originates from the monotonicity of $t_0(t_E)$, the second

from $t_0 \sim t_*$ and $t_* \ll t_\Lambda$. The comoving radius at t_0 is

$$\begin{aligned}\xi(t_0) &= \xi_{max} - \int_0^{t_0} \frac{d\bar{a}}{\sqrt{t_c^2 + \bar{a}^2 + \bar{a}^4/t_\Lambda^2}} \\ &\sim \xi_{max} - \int_{t_c}^{t_0} \frac{d\bar{a}}{\bar{a}} \\ &\sim \xi_{max} - \ln t_0/t_c \end{aligned} \tag{4.64}$$

and hence the area of the apparent horizon will be

$$A_{AH} \sim t_0^2 \, e^{2(2\xi_{turn} - \ln t_0/t_c)} \sim \Lambda^{-2} t_c^{-2} \tag{4.65}$$

We therefore find $S_{max}/A_{AH} \sim t_c^{-1/2}$, which is consistent with what we found previously, considering $S_{max} \sim S(L_{out})$.

4.5 Gravitational Collapse

In the previous sections we considered several cosmological examples. However, the initial conditions of all those consisted of many causally disconnected regions near to the big bang. It is hence impossible to find a future light-cone of an observer containing all those regions. Therefore, in this section we will describe some examples that do exist in such a future light-cone, and can hence be created by an experimentalist starting in flat space.

4.5.1 Collapsing Ball of Dust

Consider again the situation of section 4.3.1, for the case of pressureless matter. In the far future, the matter density becomes increasingly dilute and the open FRW space becomes increasingly flat, approaching flat Minkowski. Imagine that now we reverse the time for that solution, then we start from a flat Minkowski. The observer in the previous section, that had a past light-cone containing the saturating light-sheet, will now become an observer with a future directed light-cone containing a saturating light-sheet. This is exactly the situation we were looking for.

Consider a pressureless dust ball, in fact the time-reversed cosmology, with maximal comoving radius ξ_{max}. Outside we assume vacuum. The metric outside will be that of the Schwartzschild black hole metric, as dictated by the Birkhoff theorem,

$$ds^2 = -\left(1 - \frac{2M}{r}\right) d\tau^2 + \left(1 - \frac{2M}{r}\right)^{-1} dr^2 + r^2 d\Omega^2 \tag{4.66}$$

We now have to find the relation between the Schwarzschild variables (M, r, τ) the cosmological variables (t_c, ξ, t), describing the space outside and inside the dust ball respectively. In order to do so, consider a geodesic in the cosmology at fixed ξ_{max}, on the boundary between

dust ball and vacuum space. The geodesic can be thought of as describing a dust particle on this edge, hence it should be a radial timelike geodesic both from the FRW and the Schwarzschild point of view. Furthermore, we have $d\xi = d\Omega = 0$ and hence the FRW coordinate t is the proper time along the geodesic. The following relation is then obvious,

$$dt^2 = (1 - 2M/r)d\tau^2 - (1 - 2M/r)^{-1}dr^2 \tag{4.67}$$

From equation (4.66) we see that the Schwarzschild metric is independent of τ, hence possessing a timelike Killing vector $\tau^a = \partial_\tau$. Contraction with the four-velocity v^a results in a conserved quantity,

$$\gamma = -g_{ab}\tau^a v^b = (1 - 2M/r)\delta^\mu_\tau \frac{\partial x^\mu}{\partial t} = (1 - 2M/r)\frac{\partial \tau}{\partial t} \tag{4.68}$$

Some straightforward algebra leads to a more useful reformulation of this last equation,

$$\frac{\dot{r}^2}{r^2} = \frac{2M}{r^3} + \frac{\gamma^2 - 1}{r^2} \tag{4.69}$$

For a fixed time t, all comoving geodesics at ξ_{max} form a 2-sphere with area $a(t)^2 \sinh^2 \xi_{max}$, like we have seen in the previous sections. This must be exactly the same for that surface in the Schwarzschild coordinates,

$$r(t) = a(t) \sinh \xi_{max} \tag{4.70}$$

Substitution in equation (4.69) leads to

$$\frac{\dot{a}^2}{a^2} = \frac{2M}{a^3 \sinh^3 \xi_{max}} + \frac{\gamma^2 - 1}{a^2 \sinh^2 \xi_{max}} \tag{4.71}$$

Comparing this with the Friedmann equation (4.36) reveals the relations $\gamma = \cosh \xi_{max}$ and $2M = t_c \sinh^3 \xi_{max}$.

Next, let's have a look at the ball of dust in the dilute limit, $t \to \infty,\ r \to \infty$. Both metrics approach the Minkowski metric, and we will look at the matter distribution on a slice of constant Minkowski-time. We remark first that the Schwarzschild coordinates (τ, r) approach the time and radial coordinates of Minkowski in this case, while the FRW coordinates (t, ξ) become the Milne coordinates

$$\tau = t \cosh \xi \qquad r = t \sinh \xi \tag{4.72}$$

Hence, on a slice of constant τ_0, the particles occupy a region $0 \leq r \leq r_{max}$ and move in the radial direction. The comoving geodesics are still the paths of constant ξ, thus the particles on such a slice will have a speed $v = dr/d\tau = \tanh \xi$. The conserved quantity γ now appears to be the Lorentz boost factor in this limit:

$$\tanh^2 \xi = 1 - 1/\cosh^2 \xi \quad \Rightarrow \quad \gamma^{-2} = 1 - v^2 \tag{4.73}$$

The velocity distribution is now also clear, with the help of equation (4.72) one finds $v(r) = r/\tau_0$.

The energy-momentum tensor can now easily be written in Minkowski-space coordinates, using $a(t) = t$ for the dilute limit,

$$T_{ab} = \rho dt^2 = \frac{3t_c}{8\pi}\frac{dt^2}{t^3} = \frac{3t_c}{8\pi}\frac{(\tau d\tau - r dr)^2}{(\tau^2 - r^2)^{5/2}} \tag{4.74}$$

The energy density is then the coefficient of $d\tau^2$, and the number density can be found by dividing this by the particle energy γm,

$$n(r) = \frac{1}{m\gamma}\frac{3t_c}{8\pi}\frac{\tau_0^2}{(\tau_0^2 - r^2)^{5/2}} = \frac{3t_c}{8\pi}\frac{\tau_0}{(\tau_0^2 - r^2)^2} \tag{4.75}$$

The total number of particles is

$$\begin{aligned} N &= 4\pi \int_0^{r_{mas}} \left(\frac{3t_c}{8\pi m}\frac{\tau_0}{(\tau_0^2 - r^2)^2}\right) r^2 dr \\ &= \int_0^{\xi_{max}} \frac{\tanh^2\xi}{(1-\tanh^2\xi)^2} d\tanh\xi \\ &= \frac{3t_c}{2m}\int_0^{\xi_{max}} \sinh^2\xi d\xi \\ &= \frac{3t_c}{8\pi m} V_c(\xi_{max}) \end{aligned} \tag{4.76}$$

where we made use of $\tanh\xi = r/\tau_0 = v$ and $\frac{\tau_0}{\sqrt{\tau_0^2 - r^2}} = \frac{1}{\sqrt{1-v^2}}$.

The question now is how to create this situation in Minkowski space. We will thus continue using the Minkowski coordinates to show that it is possible to find a light-sheet exceeding $S \leq A^{3/4}$. In order to do so we introduce a parameter α,

$$S = \alpha A^{3/4}, \tag{4.77}$$

and show that we can find $\alpha > \mathcal{O}(1)$.

Consider a large number of particles N, arranged in a sphere of radius r_{max} and each with a mass m. Furthermore, the initial velocities will be chosen in a way that they all converge in one single point, $v(r) \propto r$. These velocities will be near to the speed of light, and it will be convenient to use the Lorentz boost factor instead of the speed, $\gamma(r) = (1 - v(r)^2)^{-1/2}$. Let's call the boost factor for the most energetic particles $\gamma_{max} = \gamma(r_{max})$. Finally we also require the number density to be in accordance to equation (4.75), hence $n(r) \propto \gamma(r)^4$. If we suppose that $\gamma_{max} \gg 1$, equation (4.73) implies that, $\gamma_{max} = \cosh\xi_{max} \sim \sinh\xi_{max} \sim \exp(\xi_{max})/2$. From equation (4.76) we find

$$t_c = \frac{8\pi N m}{3V_c(\xi_{max})} \sim \frac{Nm}{\gamma_{max}^2} \tag{4.78}$$

Hence, for light-sheets that extend to this point in (FRW) time, the entropy will be, as calculated in section 4.3.1,

$$S \sim (mt_c)^{-1}\ A \sim \frac{\gamma_{max}^2}{Nm^2} A \tag{4.79}$$

Comparison with equation (4.77) learns

$$\alpha \sim \frac{\gamma_{max}^{3/2}}{N^{3/4} m^{3/2}} S^{1/4} \tag{4.80}$$

Fixing γ_{max}, N and m, the entropy is the only part that will be variable depending on which light-sheet we choose. Obviously we want to look at the light-sheet that will contain the most entropy, which can be maximally $S \sim N$. There is a light-sheet that will indeed have such an entropy, namely the one that starts on the apparent horizon and reaches $\xi = \xi_{max}$ at the time $t = t_c$. We then have

$$\alpha \sim \left(\frac{\gamma_{max}^3}{Nm^3} \right)^{1/2}. \tag{4.81}$$

From section 4.3.1, we know that $m > t_c^{-1/2}$ is needed for the validity of the entropy counting we used. Saturating this will lead to the maximum possible entropy-area ratio. Indeed, it then follows that $\gamma_{max}^2 \sim Nm^3$, which finally gives

$$\alpha \sim (Nm^3)^{1/4} \sim \gamma_{max}^{1/2} \tag{4.82}$$

And since we assumed $\gamma_{max} \gg 1$, we find indeed $\alpha > \mathcal{O}(1)$.

4.6 Saturation Within a Causal Diamond

The previous examples convinced us that the bound $S \leq A^{3/4}$ is not generally valid. This doesn't mean that it cannot be valid under certain conditions. All our examples in the previous sections do not lie within a causal diamond, hence we will investigate if the naive bound can be violated for the latter situation. A causal diamond of a worldline is the region of space-time which can both receive signals from and send signals to that worldline. In other words, we will investigate the entropy of systems that can be both set up and observed by the same person.

4.6.1 Shell of Dust in AdS

The metric of the empty AdS space can be written in the following way,

$$ds^2 = -dt^2 + a^2(\tau)(d\chi^2 + \sinh^2 \chi d\Omega 2_2), \tag{4.83}$$

with $a(t) = t_\Lambda \sin(t/t_\Lambda)$. We will now add a spherically symmetric shell of dust. The density of the matter should be low, in order to be able to use the vacuum metric nonetheless. We assume the dust at rest, and this will remain so since the worldlines with constant spatial

coordinates are geodesics. Let χ_{max} and χ_{min} be the comoving radius of the boundaries of the shell.

Let's consider the condition on the density of the dust. We require it to be only a small perturbation at the turnaround time $t = t_\Lambda \pi/2$, which implies that the density should be negligible compared to the vacuum energy,

$$\rho_m \ll \frac{1}{t_\Lambda} \tag{4.84}$$

At the turnaround time, the scale factor is maximal. This means that the dust will follow converging geodesics, and the probe approximation will not be valid any longer. The metric in the dust shell will only be approximated by (4.83) as long as the matter density obeys (4.84).

Let's now calculate the future directed ingoing light-sheet. The past directed ingoing light-sheet can be calculated in the same way, since the space-time is symmetric about the turnaround time. Hence, if we find that they reach the origin, the matter is contained in the causal diamond of the observer in the origin. The radial light rays are given by

$$d\chi = \frac{dt}{a(t)} \tag{4.85}$$

which can be rewritten using $\dot{a}^2 = 1 - \frac{a^2}{t_\Lambda^2}$,

$$d\chi = \frac{da}{a\sqrt{1 - a^2/t_\Lambda^2}} \tag{4.86}$$

Integrating equation (4.86) leads to

$$\Delta\chi = \cosh^{-1}\left(\frac{t_\Lambda}{a}\right) \tag{4.87}$$

From this equation, it follows that the light will travel one comoving radius $\Delta\chi = 1$ in the time that the scale factor a decreases a few times smaller than t_Λ, and the density increases as $\rho_m \sim a^{-3}$. Hence, if we choose the shell extend over one comoving radius, and if we suppose the initial matter density to be a lot less than the vacuum energy, our probe approximation remains valid until the light-sheet escapes from the shell. The light-sheet will now certainly reach the origin: the metric inside the shell is the vacuum AdS metric, and the dust particles at the inner boundary of the shell will follow a timelike geodesic. The light rays, following null geodesics, are thus certain to reach the origin before the metric would be affected by the collapsing matter.

We will now calculate S/A for the previous light-sheet. Suppose the matter to be nearly relativistic, then the relation between entropy density and matter energy density is

$$s \sim \rho_m^{3/4} \tag{4.88}$$

The entropy will then be bounded below by the entropy on the spatial slice at the turnaround time, which has maximal expansion coefficient. The entropy on this spatial slice is, using $\Delta\chi = 1$ and $a = t_\Lambda$ at the turnaround time,

$$S = sV = \rho_m^{3/4} A t_\Lambda \tag{4.89}$$

Finally, to remain in the probe approximation, we have $\rho_m < \rho_\Lambda$. The entropy-area ratio will therefore be

$$S/A \leq t_\Lambda^{-3/2} t_\Lambda \leq t_\Lambda^{-1/2} \tag{4.90}$$

For a large comoving radius ξ, one can obtain $A \gg \Lambda^{-1}$ and therefore a light-sheet with $S \gg A^{3/4}$ within a causal diamond.

4.6.2 Slow Feeding of a Black Hole

Let's consider a black hole of radius R. Imagine we send massless quanta into this black hole, one at the time. The wavelength of each quantum is λ, and the energy is λ^{-1}. Hence the black hole will have doubled his energy and radius after $R\lambda$ quanta have been absorbed. The area of the black hole horizon will now be $4\pi(2R)^2$. This surface possesses a past-directed ingoing light-sheet which coincides with that part of the event horizon that absorbed the $R\lambda$ quanta. The light-sheet will therefore have an entropy of order $R\lambda$, the number of quanta that crosses the light sheet one by one. We therefore find the ratio

$$\frac{S}{A} \sim \frac{\lambda}{R} \tag{4.91}$$

We first remark that the covariant bound will not be violated, since the quanta with wavelengths $\lambda \gg R$ will not be absorbed by the black hole. In the limit $\lambda \to R$, we see that the bound can be saturated, and if we choose quanta with $\lambda \gg R^{1/2}$, the bound $S \leq A^{3/4}$ is violated.

For an observer at a fixed radius outside the black hole, the light-sheet discussed in this example is part of the boundary of this observer's causal diamond. Hence, this example shows that a light-sheet with $S \gg A^{3/4}$ can exist within a causal diamond.

Chapter 5

Bianchi Type I model

In the previous chapter, several examples were found that violate the naive bound $S < A^{3/4}$, and some that even saturate the CEB. These examples differ from previous work in the fact that they consider cosmologies with a physical matter content and observable light-sheets. In this chapter, we will proceed in an analogous way, but our model under consideration will be anisotropic. Our goal will be to find more examples that violate $S < A^{3/4}$, considering a dust-filled universe. In the next chapter we will repeat this exercise for an inhomogeneous model.

Consider the Bianchi type I universe model, which has the following metric:

$$ds^2 = -\,dt^2 + X^2(t)\,dx^2 + Y^2(t)\,dy^2 + Z^2(t)\,dz^2 \tag{5.1}$$

This model describes the simplest anisotropic generalisation of the flat FRW models. Spatially, these models are homogeneous. The average expansion scale factor is given by

$$S(t) = (XYZ)^{1/3} \tag{5.2}$$

The generalized Friedmann equation is[9]

$$3\frac{\dot{S}^2}{S^2} = \frac{\Sigma^2}{S^6} + \frac{M}{S^{3\gamma}} \tag{5.3}$$

where γ is determined by the perfect fluid equation of state between the fluid's pressure p and density μ,

$$p = (\gamma - 1)\mu, \quad \dot{\gamma} = 0 \tag{5.4}$$

and M is given by

$$\mu = \frac{M}{S^{3\gamma}}, \quad \dot{M} = 0 \tag{5.5}$$

A tetrad can be found by

$$e^i_\alpha = \xi^{-1}_\alpha \delta^i_\alpha \tag{5.6}$$

where $\xi_0 = 1, \xi_1 = X(t), \xi_2 = Y(t), \xi_3 = Z(t)$. The tetrad should obey[9]

$$[e_\alpha, e_0] = \left(\frac{\dot{S}}{S} \delta_\alpha^\beta + \sigma_\alpha{}^\beta \right) e_\beta \tag{5.7}$$

where σ_α^β is the shear tensor, which describes the rate of distortion of the matter flow. This tensor will satisfy[9]

$$\sigma_{\alpha\beta} = \frac{\Sigma_{\alpha\beta}}{S^3}, \quad \sigma^2 = \frac{\Sigma^2}{S^6}, \quad \Sigma^2 = \frac{1}{2}\Sigma_{\alpha\beta}\sigma^{\alpha\beta} \tag{5.8}$$

with Σ_α^β a constant tensor. From equation (5.7) we find

$$\begin{aligned} & 0 - e_0 e_\alpha = \frac{\dot{S}}{S} e_\alpha + \sigma_\alpha{}^\beta e_\beta \\ \Rightarrow \quad & \frac{\dot{\xi}_\alpha}{\xi_\alpha^2} \frac{\partial}{\partial \xi_\alpha} = \frac{\dot{\xi}_\alpha}{\xi_\alpha} e_\alpha = \frac{\dot{S}}{S} e_\alpha + \sigma_\alpha{}^\beta e_\beta \\ \Rightarrow \quad & \frac{\dot{\xi}_\alpha}{\xi_\alpha} \delta_\alpha{}^\beta = \frac{\dot{S}}{S} \delta_\alpha{}^\beta + \sigma_\alpha{}^\beta \end{aligned} \tag{5.9}$$

Hence, the non-vanishing components of the shear tensor are

$$\sigma_{11} = \frac{\dot{X}}{X} - \frac{\dot{S}}{S}, \quad \sigma_{22} = \frac{\dot{Y}}{Y} - \frac{\dot{S}}{S}, \quad \sigma_{33} = \frac{\dot{Z}}{Z} - \frac{\dot{S}}{S} \tag{5.10}$$

We will now calculate $X(t)$, and the other scale factors can be calculated analogously. Suppose the function $X(t)$ is of the form $X(t) = S(t)\, f(t)$, with f a function to be determined. Writing $\Sigma_{11} = \Sigma_1$, equations (5.8) and (5.10) then imply

$$\frac{\dot{f}}{f} = \frac{\Sigma_1}{S^3} \quad \Rightarrow \quad f = \exp\left(\Sigma_1 \int \frac{dt}{S^3} \right) \tag{5.11}$$

Hence, the individual length scales are given by

$$X(t) = S(t) \exp(\Sigma_1 W(t)), \quad Y(t) = S(t) \exp(\Sigma_2 W(t)), \quad Z(t) = S(t) \exp(\Sigma_3 W(t)) \tag{5.12}$$

with $W(t) = \int \frac{dt}{S^3(t)}$ and

$$\Sigma_1 + \Sigma_2 + \Sigma_3 = 0, \quad \Sigma_1^2 + \Sigma_2^2 + \Sigma_3^2 = 2\Sigma^2 \tag{5.13}$$

From equation (5.12) we can see that the case in which $\Sigma = 0$ would correspond to the isotropic case. The solution to equations (5.13) is given by

$$\Sigma_\alpha = (2\Sigma/\sqrt{3}) \sin \alpha_\alpha, \quad \alpha_1 = \alpha, \quad \alpha_2 = \alpha + 2\pi/3, \quad \alpha_3 = \alpha + 4\pi/3 \tag{5.14}$$

with α a constant.

In the case of dust, we have $\gamma = 1$, and it follows from the Friedmann equation (5.3) that

$$\begin{aligned} & \frac{1}{3}\frac{\dot{S}^3}{S^3} = \frac{\dot{S}}{S} = \frac{\Sigma^2}{S^6} + \frac{M}{S^{3\gamma}} \\ \Rightarrow \quad & \frac{d(S^3)}{\sqrt{\Sigma^2/M + S^3}} = \sqrt{3M}dt \\ \Rightarrow \quad & \sqrt{\Sigma^2/M + S^3} = \frac{\sqrt{3M}}{2}t + C \\ \Rightarrow \quad & S(t) = (\frac{3}{4}Mt^2 + \sqrt{3}\Sigma t)^{1/3} \end{aligned} \tag{5.15}$$

were we determined the integration constant $C = \sqrt{\Sigma^2/M}$ such that the average expansion factor S is zero when $t = 0$. From $W = \int dt/S^3$ it is then easy to find

$$W(t) = \frac{1}{\sqrt{3}\Sigma} \ln\left(\frac{t}{\frac{3}{4}Mt + \sqrt{3}\Sigma}\right), \tag{5.16}$$

which finally leads to

$$X(t) = S(t)\left(\frac{t^2}{S(t)^3}\right)^{\frac{2}{3}\sin\alpha_1}, \quad Y(t) = S(t)\left(\frac{t^2}{S(t)^3}\right)^{\frac{2}{3}\sin\alpha_2}, \quad Z(t) = S(t)\left(\frac{t^2}{S(t)^3}\right)^{\frac{2}{3}\sin\alpha_3} \tag{5.17}$$

We will consider the case in which two coordinate directions have the same length scale. From equation (5.17) we see that such cases occur when $\alpha = \pi/2$ or $\alpha = \pi/6$. We will use the former, but the latter is analogous. Hence, using $\alpha = \pi/2$ we get

$$X(t) = \frac{t^{4/3}}{S(t)}, \quad Y(t) = Z(t) = S^2(t)t^{-2/3} = \frac{t^2}{X^2(t)} \tag{5.18}$$

For simplicity, let's rewrite some of the previous equations in our specific case of dust-filled Bianchi type I cosmology. The metric is

$$ds^2 = -dt^2 + X^2(t)dx^2 + Y^2(t)(dy^2 + dz^2) \tag{5.19}$$

with $X(t)$ and $Y(t)$ given by (5.18). The average scale factor is

$$S^3(t) = \sqrt{3}\Sigma t\left(\frac{t}{t_M} + 1\right) \tag{5.20}$$

where

$$t_M = \frac{4}{\sqrt{3}}\frac{\Sigma}{M} \tag{5.21}$$

We will now consider a surface around the origin in the (yz)-plane: let's choose a disk of proper area

$$A = 4\pi r^2 Y^2(t_0) \tag{5.22}$$

where $r^2 = y^2 + z^2$.

5.1 Case 1

Suppose we have

$$1 \ll t_0 \ll t_M \tag{5.23}$$

to leading order in t, we find

$$\begin{aligned} S(t) &\sim \left(\sqrt{3}\Sigma\right)^{1/3} t^{1/3} \\ X(t) &\sim \left(\sqrt{3}\Sigma\right)^{-1/3} t \\ Y(t) &\sim \left(\sqrt{3}\Sigma\right)^{2/3} \left(\frac{t}{t_M} + 1\right) \end{aligned} \tag{5.24}$$

The light-sheet will consist of light-rays normal to this surface. From (5.24) we see that in this regime, $t/t_M \ll 1$, the scale factor $Y(t)$ is approximately constant. Parallel light-rays emanating from the surface will therefore remain parallel, and the expansion of the light-sheet will be vanishing. Consider for example a past directed light-sheet in the direction of increasing x,

$$\begin{aligned} &\frac{1}{X(t)} dt = dx \\ \Rightarrow &\left(\sqrt{3}\Sigma\right)^{1/3} \frac{dt}{t} = dx \\ \Rightarrow &\left(\sqrt{3}\Sigma\right)^{1/3} \ln\left(\frac{t_0}{t_1}\right) = x_1 - x_0 \end{aligned} \tag{5.25}$$

with $t_0 > t_1$ since it is past-directed.

The comoving volume of the light-sheet is

$$\begin{aligned} V_c &\sim r^2 \Delta x \\ &\sim r^2 \left(\sqrt{3}\Sigma\right)^{1/3} \ln\left(\frac{t_0}{t_1}\right) \\ &\sim r^2 \left(\sqrt{3}\Sigma\right)^{1/3} \ln t_0 \end{aligned} \tag{5.26}$$

where in the last step we assumed the light-sheet to continue until $1 \leq t_1 \ll t_0$. Assuming the comoving entropy density for dust to be equal to the number density, $\sigma = M/m$, with M the total mass per comoving unit volume and m the mass of one dust particle, the total entropy on the light-sheet will be

$$S \sim \sigma V_C \sim r^2 \left(\sqrt{3}\Sigma\right)^{1/3} \ln t_0 \frac{M}{m} \tag{5.27}$$

From equation (5.22), the area of our initial surface is

$$A \sim r^2 \left(\sqrt{3}\Sigma\right)^{4/3} \tag{5.28}$$

Hence, we find an entropy/area ratio equal to

$$\frac{S}{A} \sim \frac{1}{m} \frac{\ln t_0}{t_M} \tag{5.29}$$

For large enough comoving coordinates y and z, the bound $S \leq A^{3/4}$ can be violated. This can be achieved choosing

$$r^{1/2} \gg \frac{\Sigma^{2/3}}{\sigma \ln t_0}, \tag{5.30}$$

The covariant bound will still hold, since the formula for the entropy density to be equal to the number density is only valid when the number density is less than one particle per Compton wavelength cubed, resulting in

$$m^4 > \mu \sim \frac{M}{S^3} \sim (t t_M)^{-1} \tag{5.31}$$

This should be hold in the interval $1 < t < t_M$, hence $m > t_M^{-1/4}$. The largest entropy/area ratio for this case will then approximately be $S/A \sim t_M / \ln(t_M) < 1$.

5.2 Case 2

Suppose $1 < t_M \ll t_0$. In this regime, the scale factors can be approximated by

$$\begin{aligned} S(t) &\sim \left(\frac{\Sigma}{t_M}\right)^{1/3} t^{2/3} \\ X(t) &\sim \left(\frac{\Sigma}{t_M}\right)^{-1/3} t^{2/3} \\ Y(t) &\sim \left(\frac{\Sigma}{t_M}\right)^{2/3} t^{2/3} \end{aligned} \tag{5.32}$$

The light-rays start parallel and will diverge due to the expansion of the universe orthogonal to the x-dimension. Hence light-sheets should be past-directed, in order to have a negative expansion. The equation of a past directed light-sheet, in the direction of decreasing x coordinate, is

$$\begin{aligned} &\frac{dt}{X(t)} = dx \\ \Rightarrow &3 \left(\frac{t_M}{\sqrt{3}\Sigma}\right)^{-1/3} (t_0^{1/3} - t_1^{1/3}) = x_0 - x_1 \end{aligned} \tag{5.33}$$

The comoving volume of the light-sheet is

$$V_c \sim \Delta x \; r^2 \sim r^2 \; \left(\frac{t_M}{\Sigma}\right)^{-1/3} (t_0^{1/3} - t_1^{1/3}) \tag{5.34}$$

We can now calculate the entropy on the light-sheet, using $\sigma = M/m$,

$$S \sim \sigma V_c \sim r^2 \sigma (\Sigma/t_M)^{1/3} t_0^{1/3}, \tag{5.35}$$

assuming the light-sheet extending until $t_M \ll t_1 \ll t_0$. The area of the initial surface is equal to $A \sim r^2 (\Sigma/t_M)^{4/3} t_0^{4/3}$, hence

$$\frac{S}{A} \sim \frac{1}{m\ t_0} \tag{5.36}$$

Choosing $r \gg \frac{(Mt_0)^{4/3}}{\sigma^2}$, the naive bound $S \leq A^{3/4}$ will be violated. The same argument as the one we mentioned in the end of section (5.1) can be used to show the covariant bound holds, and since $t_0 \gg 1$, the light-sheet will not be able to saturate the CEB.

A major remark is that the stronger bound (3.9) should be considered in both previous cases. In the first case, the derivation should still hold if were able to neglect the entropy contribution of the part of the light-sheet that continues until $t = 0$. However our approximation is not suitable to calculate such a light-sheet. In the case we apply the stronger bound (3.9), than we should keep the t/t_M term in equation (5.24), resulting in $A(t_0) - A(t_1) \sim r^2\,(\Sigma)^{4/3}\, t_0/t_M$. This leads to the fact that the CEB only holds if

$$\frac{t_0}{\ln t_0} > t_M^{1/4} \tag{5.37}$$

The entropy bound would be violated otherwise, and we could argue that in (a part of) this regime, $t < t_M$, a quantum gravitational description is still needed. From equation (5.24) we can indeed see that if $t \ll t_M$, at least for the y and z dimensions the situation is not much different then for the big bang $t = 0$. Provided that, for large enough t_0 such that equation (5.37) is satisfied as well as the other requirements of section (5.1), the above derivation would still hold. Then this case shows a new way of violating $S < A^{3/4}$ since it would be only possible for this anisotropic model. Indeed, the time t_M and hence the regime under consideration does not exist in isotropic models.

In the second case, the derivation presented is a good approximation even for the stronger bound (3.9) since $A(t_0) - A(t_1) \sim A(t_0)$. From equation (5.17), we see that at late times the universe isotropizes. Hence this case should not be restricted to only anisotropic models.

Chapter 6

Lemaitre-Tolman-Bondi model

Consider the case of a spherically symmetric inhomogeneous model of the universe. The metric of such a model describing a dust-filled universe in matter-comoving coordinates is

$$ds^2 = -dt^2 + \frac{(Y'(t,r))^2}{1+2E(r)}\, dr^2 + Y^2(t,r)d\Omega^2 \tag{6.1}$$

This is the Lemaitre-Tolman-Bondi metric, with $d\Omega^2 = d\theta^2 + \sin^2\theta\ d\phi^2$ and $Y(t,r)$ obeying a generalized Friedmann equation,

$$\dot{Y}(t,r) = \pm\sqrt{\frac{2M(r)}{Y(r,t)} + 2E(r)} \tag{6.2}$$

We use the convention that a dot represents the partial time derivative $\partial/\partial t$, while a prime stands for the partial radial derivative $\partial/\partial r$. The energy density is determined by

$$4\pi\ \mu(t,r) = \frac{M'(r)}{Y^2(t,r)Y'(t,r)} \tag{6.3}$$

Equation (6.2) has the solution [9]

$$Y(t,r) = \frac{M(r)}{\mathcal{E}(r)}\phi_0(t,r), \quad \xi(t,r) = \frac{(\mathcal{E}(r))^{3/2}\,(t - t_B(r))}{M(r)} \tag{6.4}$$

with

$$\mathcal{E}(r) = \begin{cases} 2E(r) \\ 1 \\ -2E(r) \end{cases} \qquad \phi_0 = \begin{cases} \cosh\eta - 1 \\ (1/2)\eta^2 \\ 1 - \cos\eta \end{cases} \qquad \xi = \begin{cases} \sinh\eta - \eta \\ (1/6)\eta^3 \\ \eta - \sin\eta \end{cases} \qquad \text{when} = \begin{cases} E > 0 \\ E = 0 \\ E < 0 \end{cases} \tag{6.5}$$

with $\eta = \eta(t,r)$ a parameter. The model is characterized by the three arbitrary functions $M(r), E(r), t_B(r)$. The function $t_B(r)$ is the local time at which $Y = 0$, or in other words the time of the local big bang.

6.1 Parabolic solution

We will first consider the $E = 0$ solution of the LTB-model, which is called the parabolic solution. From equations (6.4) and (6.5) we find

$$\begin{aligned} M(r) &= \frac{6(t - t_B)}{\eta^3} \\ Y(r,t) &= M(r)\frac{\eta^2}{2} \end{aligned} \tag{6.6}$$

Eliminating the parameter η in the previous equations results in

$$Y(t,r) = \left(\frac{9}{2}M(t - t_B)^2\right)^{1/3} \tag{6.7}$$

Suppose we choose the function $t_B(r)$ to be rapidly converging to a constant C for comoving radius bigger than r_c. For example, the function

$$t_B(r) = -\frac{1}{10x + 1} + 1 \tag{6.8}$$

will be approximately equal to one for $r > 1$. Differentiating equation (6.7) with respect to r yields

$$Y' = \frac{Y}{3M}M' - \frac{2}{3}\frac{Y}{t - t_B}t_B' \tag{6.9}$$

As one can easily see, the area of a sphere centered around the origin is equal to

$$A = 4\pi Y^2 \tag{6.10}$$

Assuming this sphere well outside r_c and at a time $t_0 \gg C$, we can write

$$A \sim M^{2/3}(r_0)\tau_0^{4/3} \tag{6.11}$$

where $\tau = t - C$. Let's now suppose r_c is sufficiently small, such that $M(r_c) << M(r_0)$. The volume of a sphere from t_c to t_0 is then

$$\begin{aligned} V &\sim 4\pi \int_{r_c}^{r_0} Y^2 Y' dr \\ &\sim \frac{4}{3}\pi \int_{M_c}^{M_0} \frac{Y^3}{M} dM \\ &\sim \frac{4}{3}\pi\frac{9}{2}\tau_0^2(M_0 - M_c) \\ &\sim \tau_0^2 M_0 \end{aligned} \tag{6.12}$$

where we used $t_B' \sim 0$. Combining equation (6.9) without the last term, which should be a good approximation for the region $r > r_c$, with equation (6.3) leads to

$$\frac{4}{3}\pi Y^3 \mu \sim M \tag{6.13}$$

which shows that $M(r)$ can be approximately interpreted as the total mass within a sphere of radius r.

Radial light rays in the region $r > r_c$ will obey

$$\begin{aligned} &\Rightarrow dt = Y' dr \\ &\Rightarrow dt = \frac{YM'}{3M} dr \\ &\Rightarrow dt \propto M^{-2/3} \tau^{2/3} dM \\ &\Rightarrow \tau^{1/3} \propto M^{1/3} \end{aligned} \tag{6.14}$$

Let's choose the initial sphere bigger than the particle horizon, $M_0 \gg \tau_0$. The generating light-rays for a past, ingoing light-sheet will then obey

$$\tau_0^{1/3} - \tau_1^{1/3} \propto M_0^{1/3} - M_1^{1/3} \tag{6.15}$$

where we neglected order one factors. Assuming that the light-sheet extends sufficiently into the past to obtain $\tau_1 \ll \tau_0$ while staying well outside the sphere of radius r_c, we find

$$\begin{aligned} M_1 &\sim M_0 \left(1 - (\frac{\tau_0}{M_0})^{1/3}\right)^3 \\ \Rightarrow M_1 &\sim M_0 - 3\tau_0^{1/3} M_0^{1/3} \end{aligned} \tag{6.16}$$

The entropy density is approximated by the number density of the dust particles. The total entropy on the light-sheet we constructed above, will then be

$$S = \frac{M_0 - M_1}{m} \tag{6.17}$$

with m the mass of a single dust particle. Combining equations (6.16) and (6.17), we find

$$S \sim \frac{t_0^{1/3} M_0^{2/3}}{m} \tag{6.18}$$

Dividing the entropy by the area of the surface (6.11), finally leads to

$$\frac{S}{A} \sim \frac{1}{m t_0} \tag{6.19}$$

The covariant bound will indeed hold: the formula for the entropy density to be equal to the number density is only valid when the number density is less than one particle per Compton wavelength cubed, resulting in

$$\begin{aligned} & m^4 > \mu \sim M/Y^3 \sim t^{-2} \\ \Rightarrow \quad & m > t^{-1/2} \end{aligned} \tag{6.20}$$

This should hold for the whole time interval $1 < t_1 < t < t_0$, hence $m > t_1^{-1/2} \gg t_0^{-1/2}$ and therefore $mt_0 > 1$. Secondly, by choosing a large enough radius, the naive bound $S < A^{3/4}$ will be violated. Indeed,

$$\begin{aligned} & S \sim \frac{M_0^{1/6}}{mt_0^{2/3}} A^{3/4} \\ \Rightarrow \quad & S \gg A^{3/4} \qquad \text{if we choose } M_0 \gg m^6 t_0^4 \end{aligned} \tag{6.21}$$

One way to interpret this result is to remark that, in the regime $r > r_c$ which we considered, the spacetime behaves as a flat FRW universe. Since our case is very similar to that of truncated light-sheets, our result is somehow expected to violate $S < A^{3/4}$.

6.2 Hyperbolic solution

A second family of solutions of the LTB equations (6.4) and (6.5), with positive $E(r)$, is called hyperbolic. In this and the next section we will consider a simultaneous big bang time for all values of comoving radius r, $t_B = \text{constant} = 0$.The solution we will consider is

$$\begin{aligned} Y(r,t) &= B\ a(t)\ \exp[R(r+\frac{1}{r})] \\ M(r) &= C\ \exp[3R(r+\frac{1}{r})] \\ E(r) &= D\ \exp[2R(r+\frac{1}{r})] \end{aligned} \tag{6.22}$$

where B,C,D and R are constants, which we will choose positive in this section. This solution is indeed consistent with equations (6.4) and (6.5), if we set

$$\sinh\eta - \eta = t, (\quad \cosh\eta - 1)\dot{\eta} = 1, \dot{\eta} = a^{-1}(t) \tag{6.23}$$

The function $a(t)$ can be determined by substituting our solution into the Friedmann equation (6.2),

$$\frac{da}{\sqrt{\frac{C}{Ba} + D}} = \frac{\sqrt{2}}{B} dt \tag{6.24}$$

We will assume $a(t)$ to be positive for all $t > 0$, hence $Y(r,t)$ will be a positive function. Let us substitute $a(t) = \tau^2(t)$ and $C/(BD) = F$ in equation (6.24), which results in

$$\int \frac{\tau^2 d\tau}{\sqrt{F+\tau^2}} = \int \frac{\sqrt{D/2}}{B} dt \tag{6.25}$$

which results in

$$\frac{1}{2}\tau\sqrt{F+\tau^2} + \frac{F}{2}\ln\left(\frac{F}{\tau+\sqrt{F+\tau^2}}\right) = \frac{\sqrt{D/2}}{B} t \tag{6.26}$$

One initial condition we can require is that $Y(r,t)$ vanishes on the big bang time $t=0$, which leads to $\tau = 0$ and $F = 1$. The second term in the left hand side of equation (6.27) will be negligible, hence the function $a(t)$ can be approximated very well by

$$a + a^2 \sim \frac{2D}{B^2}t^2 \tag{6.27}$$

6.2.1 Anti-Trapped Spheres

We will first investigate the case of a sphere bigger then the apparent horizon. For simplicity, we will set the all the constants B,C,D and R equal to 1. To avoid the need for a quantum gravitational description, we will assume $t \gg 1$, hence using equation (6.27) we can make the following approximation: $a \sim t(\sqrt{2})$. Analogous to our derivation in section (4.3), the apparent horizon is determined by

$$\frac{\dot{a}}{a} = \pm\frac{\dot{f}}{f} \tag{6.28}$$

with $f = \exp(r + \frac{1}{r})$. This leads to

$$(1 - 1/r^2)dr = dt/t \quad \Rightarrow \quad \ln t = r + 1/r \tag{6.29}$$

We see that, for every $t > e^2 \sim 7,4$, there are two apparent horizons: one for $r_{AH,1} > 1$ and one for $r_{AH,2} = \frac{1}{r_{AH,1}} < 1$, hence resulting in two anti-trapped regions (i.e. $r > r_{AH,1}$ and $r < r_{AH,2}$). For smaller times, all spheres are anti-trapped. However, let's remark that this apparent horizon is a bad approximation for these smaller times: equation (6.29) does not specify a relation between time and comoving radius for light rays, and since we made use of $a \sim t$ which is only valid for $t \gg 1$. The particle horizon is given by

$$dt \sim t(1 - \frac{1}{r^2})dr \quad \Rightarrow \quad \ln t \sim r + \frac{1}{r} \tag{6.30}$$

where we used the approximation

$$\frac{\exp[R(r + \frac{1}{r})](1 - \frac{1}{r^2})}{\sqrt{1 + 2\exp[2R(r + \frac{1}{r})]}} \sim \frac{(1 - \frac{1}{r^2})}{\sqrt{2}} \tag{6.31}$$

The apparent horizon and the particle horizon are thus equal, at least in our approximation for large times.

Consider now a sphere at radius $r_0 \gg \ln t_0 \gg 1$, well outside the biggest apparent horizon. Analogous to the previous chapter, we will investigate the past outgoing light-sheet. The light-rays generating this light-sheet obey:

$$\ln(t_0/t_1) = r_1 - r_0 \tag{6.32}$$

Suppose t_0 sufficiently large, and imagine we end the light-sheet at an early time, such that $t_0 \gg t_1 > 1$, then we have $r_1 \gg r_0 > 1$. The comoving volume of a sphere is $V_c = V/S^3$ where $S = \frac{Y'}{\sqrt{1+2E}}$. Using the approximation (6.31), we get

$$\begin{aligned} V_c &= 4\pi \frac{\int Y^2 \frac{Y'}{\sqrt{1+2E}}}{S^3} \\ \Rightarrow \quad V_c &\sim \frac{\exp(2r + 2/r)}{(1 - 1/r^2)^3} \end{aligned} \tag{6.33}$$

Using this result, the comoving volume of a the light-sheet becomes $V_c \sim V_c(r_1) - V_c(r_0) \sim V_c(r_1) \sim \exp(2r_1)$. The entropy on the light-sheet is

$$S \sim \sigma \exp(2r_1) \sim \sigma \exp(2r_0) \frac{t_0^2}{t_1^2} \tag{6.34}$$

where we used equation (6.32). The area of the initial surface is $A \sim a_0^2 \exp(2r_0) \sim t_0^2 \exp(2r_0)$, which leads us to

$$\frac{S}{A} = \frac{\sigma}{t_1^2} \tag{6.35}$$

If the we maximize the comoving entropy density $\sigma \to 1$ and the light-sheet $t_1 \to 1$, we see that the covariant entropy bound can be saturated, but not violated. A remark is that in our derivation of equation (6.35) we neglected the contribution to the entropy for times near the big bang. One way to interpret this result, is by remarking that in the limit $r > 1$, $t > 1$, the model is very close to an open FRW universe with zero cosmological constant. Indeed, in this limit we have $Y \sim a \exp(r)$ and the metric can be approximated as

$$ds^2 = -dt^2 + a^2 \left(\frac{d(\exp r)^2}{1 + 2\exp(2r)} + \exp(2r) d\Omega^2 \right) \tag{6.36}$$

Let's now investigate the light-sheets for spheres smaller than the inner apparent horizon. Let's assume we will only look at the region of spacetime with $1/r >> 1$, then the metric can be approximated by

$$ds^2 = -dt^2 + \frac{a^2 \exp(2/r)}{r^4(1 + \exp(1 + 2/r))} dr^2 + a^2 \exp(2/r) d\Omega^2 \tag{6.37}$$

After substituting $1/r = \xi$, we will again find the metric of an open FRW universe with zero cosmological constant. Therefore, an analysis analogous to the one for the outer apparent horizon can be repeated in this regime, and will result in a similar conclusion. The solution under consideration can hence be regarded as a union of two flat FRW spacetimes.

6.2.2 Truncated Light-Sheets

Because the particle horizon and the apparent horizon are approximately equal, the same spheres we considered in the previous section will have truncated past directed ingoing light-sheets. Consider now a sphere at radius $r_0 \gg \ln t_0 \gg 1$, well outside the particle horizon.

The analysis is similar to the calculations in the previous section, resulting in:
the light-rays generating such a light-sheet obey

$$\ln(t_0/t_1) = r_0 - r_1 \tag{6.38}$$

The comoving volume of the light-sheet will be approximately $V_c \sim \exp(2r_0)$. The area of the initial surface is $A \sim a_0^2 \exp(2r_0) \sim t_0^2 \exp(2r_0)$, which leads us to

$$\frac{S}{A} = \sigma \frac{1}{t_0^2} \tag{6.39}$$

Because $t_0 > 1$ (and $\sigma \leq 1$), the covariant bound will not be violated or even saturated by this light-sheet. However, our choice of a sphere much bigger than the particle horizon, for example $r_0 \gg \ln(t_0/\sigma^2)$, leads to

$$A^{1/4}\sigma/t_0^2 \sim \sigma t_0^{-3/2} e^{r_0/2} \gg t_0^{-1} \gg 1 \tag{6.40}$$

which shows that the naive bound $S \leq A^{3/4}$ can indeed be violated.

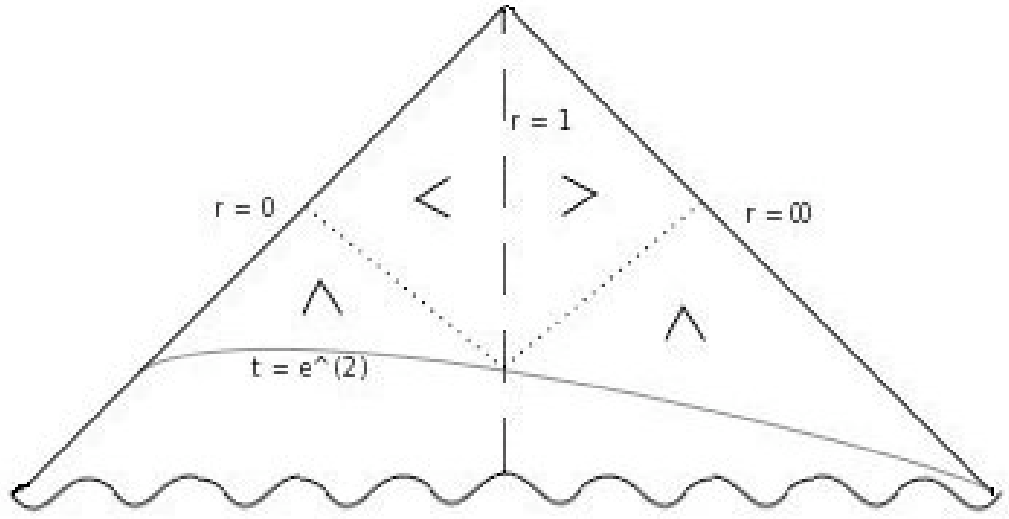

Figure 6.1: A possible Penrose diagram for the hyperbolic solution from section (6.2).

6.3 Elliptic solution

The elliptic solutions to the LTB model are those with $-1/2 \leq E(r) < 0$. A solution that would be compatible with equations (6.4) and (6.5) is for example

$$Y = a(t)\exp(-r), \quad M = \exp(-3r), \quad E = -\frac{1}{3}\exp(-2r) \tag{6.41}$$

The Friedmann equation for this solution is

$$\dot{a} = \sqrt{\frac{2}{a} - 2/3} \tag{6.42}$$

which leads to

$$\begin{aligned} & \frac{da}{\sqrt{3/a-1}} = \sqrt{2/3}dt \\ \Rightarrow \quad & \frac{\sqrt{3\tau-1}}{\tau} + 3\arctan\left(\sqrt{3\tau-1}\right) = -\sqrt{2/3}t \\ \Rightarrow \quad & 3\arctan\left(\sqrt{3\tau-1}\right) \sim -\sqrt{2/3}t \end{aligned} \tag{6.43}$$

where we substituted $a = \tau^{-1}$ in the first line and used $t > 1$ to make the approximation in the third line. This results in

$$a \sim \cos^2(Ct) \tag{6.44}$$

with C an order one constant. Using the approximation

$$\frac{Y'}{\sqrt{1+2E}} \sim -a\exp(-r) \tag{6.45}$$

we find that radial light rays obey

$$\tan(t) \sim \exp(-r) \tag{6.46}$$

From equation (6.44) we see that the function $a(t)$ becomes zero in at periodic times. However, for very small $a(t)$ we approach the quantum gravitational regime, and hence the amount of time the generating light-rays can travel is small. Indeed, the maximum for $a(t) = \cos^2(t)$ lies on $t = 0+n\pi$, but $\tan(t)$ varies slowly around this value. This implies that the light rays travel only a small comoving distance in the time range allowed for a non-quantum gravitational description, justifying the approximation $V_c \sim \Delta(r)A_c \sim \Delta(r)A_0/(a_0^2\exp(-2r_0)$. Hence we find

$$\frac{S}{A} \sim \Delta(r)\frac{e^{2r_0}}{a_0^2} \tag{6.47}$$

Even though $\Delta(r)$ is small, for large enough r_0 we see that the covariant bound can be violated. However, this violation is due to the fact that $Y(r,t)$ and $Y'/\sqrt{1+2E}$ almost vanish even for large enough r, while $a(t)$ never becomes bigger than one. Hence this spacetime is very contracted and the quantum gravitational effects are expected to be important, proving the previous calculations incorrect.

This is a general problem for solutions of the form $Y = a(t)R(r)$. Indeed, $-1/2 \leq E(r) \sim R^2(r) < 0$ requires $R^2(r)$ not to exceed a certain lower and upper boundary, hence the same can be said for $R(r)$. The Friedmann equation, in this case, will always result in $a \sim \cos^2(f(t))$

if we suppose $t > 1$, but even if we don't use this approximation a will stay remain bounded, which is clear from the Friedmann equation (6.42) itself. The limitations on $R(r)$ imply that it should be periodic or converging to a constant for $r \to \infty$. The periodic solution $R(r) = \sin(r)$ gives the closed FRW universe. Indeed, setting $E = -\sin^2(r)/2$ results in $Y'/\sqrt{1+2E} = 1$. The metric becomes

$$ds^2 = -dt^2 + a^2(t)\left(dr^2 + \sin^2(r)d\Omega\right) \tag{6.48}$$

If the $R(r)$ converges to a constant, on the other hand, for large r the spacetime converges to one constant surface. Indeed, consider a spherical surface at a time t_0 such that $a_0 > 0$. This surface has area $A = 4\pi a_0^2 R^2$. However, for large r, the area of all such surfaces is approximately equal since R is a constant. Therefore the proper distance between large comoving radii is vanishing, and a quantum gravitational description is needed.

Conclusions

The holographic principle is a remarkable property that seems to be universally valid. It relates the information content of nature to the geometry of spacetime, and therefore it seems that it originates from a yet unknown theory which unifies quantum mechanics and gravity. According to the covariant entropy bound, the amount of information that a region of space can posses is vastly less than the predictions of any current theory. Even more, it is possible that a deeper theory is not local, since the CEB states that entropy on a light-sheet is limited by the area of its boundary surface. Another interesting feature following from the holographic principle is the existence of cosmological screens. These hypersurfaces contain all the information of a spacetime, hence making it possible that our universe is a giant hologram.

Although most systems composed of ordinary matter seemed to obey a stronger bound than the CEB, $S < A^{3/4}$,counterexamples have been found by Bousso, Freivogel and Leichenauer [2] and thereby confirmed the universality of the CEB. These counterexamples can be divided in mainly two categories: truncated light-sheets and anti-trapped surfaces in open FRW universes. In the case of anti-trapped surfaces, the CEB can approximately be saturated.

New counterexamples were searched in the anisotropic Bianchi model and in the inhomogeneous LTB model. For the considered solutions of those models (except for the elliptic solution of the LTB model) counterexamples were found that are very similar to those of truncated light-sheets or anti-trapped spheres found by Bousso, Freivogel and Leichenauer [2]. One of those examples approximately saturates the CEB. A new kind of counterexample requiring anisotropy was found in the Bianchi model, but the validity of the derivation is not completely certain, since quantum gravitational effects may be important in the regime that was considered.

Appendix A

Definitions

Surface. A surface denotes a $D-2$ dimensional set of points, all of which are spacelike separated from each other. In 4 dimensional spacetime, this is what we intuitively would think of as a two dimensional surface.

Area. By area of a surface we mean the proper volume of the surface.

Hypersurface. A hypersurface H is a $D-1$ dimensional submanifold of a D-dimensional manifold M. H has $D-1$ linearly independent tangent vectors and one normal vector at any point. If the normal vector is everywhere timelike (null, spacelike), then H is called a spacelike (null, timelike) hypersurface.
We can think of a spacelike hypersurface as a snapshot of spacetime at one instant of the chosen time coordinate, and it is therefore also called timeslice. A timelike hypersurface, on the other hand, can be thought of as the history of a surface throughout time. Finally, a lightlike or null hypersurface can be built following a set of light rays emanating from each point of a surface throughout time.

Null energy condition. This energy condition demands that $T_{ab}k^a k^b \geq 0$ for all null vectors k^a. Or put in other words, light rays are focussed by matter, and not anti-focussed.

Causal energy condition. This second energy condition, $T_{ab}v^b T^{ac} v_c \leq 0$ for all timelike vectors v^a, means that energy cannot flow faster than the speed of light.

Normal surface. A closed surface that has a future-directed and a past-directed light sheet on the same side (which is called the inside).

Trapped surface A closed surface that has two future-directed light sheets.

Anti-trapped surface A closed surface that has two past-directed light sheets.

Apparent horizon. The apparent is defined geometrically as a sphere at which at least one

pair of orthogonal null congruences have zero expansion. The apparent horizon forms the boundary between a trapped or anti-trapped region and a normal region, and can have more than two light sheets.

Appendix B

Hypersurfaces

Consider a D-dimensional manifold M. One can then define a $(D-1)$-dimensional hypersurface Σ by setting a single function equal to a constant,

$$f(x) = f_* \tag{B.1}$$

We can now construct a vector field ζ^μ normal to the hypersurface, i.e. the vectorfield is orthogonal to all vectors in $T_p\Sigma \subset T_pM$ (where p is a point on Σ and T_p denotes the tangent vector space at the point p). Let's check that

$$\zeta^\mu = g^{\mu\nu}\nabla_\nu f \tag{B.2}$$

is the normal vector field. Obviously, the derivative of the function f in equation (B.2) vanishes on the hypersurface, but in general (on the manifold M) it will be different than zero, since f is a regular function on this manifold. Now, let's consider a vector $b^\mu \in T_p\Sigma$. We then find

$$b_\mu\zeta^\mu = b^\nu\nabla_\nu f \tag{B.3}$$

This time, the derivative $b^\nu\nabla_\nu$ is the directional derivative along the hypersurface. Since f is constant in that direction, equation (B.3) will always vanish and ζ^μ is indeed the normal vector field we are looking for. Moreover, the normal vector is unique up to scaling, since Σ is a codimension one hypersurface. Hence, every normal vector can be written in the form

$$\xi^\mu = h(x)\nabla^\mu f \tag{B.4}$$

for some function $h(x)$. One can then introduce a normalized normal vector n^μ, which obeys $n^\mu n_\mu = -1$ for spacelike surfaces and $n^\mu n_\mu = +1$ for timelike surfaces.

Null hypersurfaces, on the other hand, can be divided into a set of null geodesics. The union of the geodesics is the hypersurface, therefore we call them the generators of the hypersurface. A way to construct a null hypersurface is therefore to consider a (D-1)-dimensional congruence of null geodesics, which we will look into in the next appendix.

Appendix C

Geodesic congruences

To start, let us consider a one-parameter family of geodesics, $\gamma_t(\tau)$, which we have chosen in a way that the geodesics do not cross. Hence, for each $t \in \mathbb{R}$, γ_t is a geodesic parametrized by τ. Furthermore, we can choose τ and t to be the coordinates on the smooth two-dimensional surface defined by the set of these curves. One can then define two vector fields: the tangent vectors to the geodesics,

$$U^\mu = \frac{\partial x^\mu}{\partial \tau}, \tag{C.1}$$

and the deviation vectors,

$$V^\mu = \frac{\partial x^\mu}{\partial t}. \tag{C.2}$$

The vectors U and V are basis vectors of our chosen coordinate system, hence the commutator $[U, V]$ vanishes. We thus find, using the fact that the connection coefficient terms will vanish,

$$[U,V]^\mu = U^\lambda \partial_\lambda V^\mu - V^\lambda \partial_\lambda U^\mu = U^\lambda \nabla_\lambda V^\mu - V^\lambda \nabla_\lambda U^\mu = 0 \tag{C.3}$$

A congruence of geodesics is defined as a set of curves in an open region of spacetime such that every point in the region lies precisely on one curve. This means that, if the geodesics cross, the congruence will end at that point. Let now the vector $U^\mu = \frac{\partial x^\mu}{\partial \tau}$ be a tangent vector field to a four dimensional timelike geodesic congruence. This tangent vector field is normalized

$$U_\mu U^\mu = -1. \tag{C.4}$$

Further, as in equation (C.2), we consider the deviation vector V^μ, which points from one geodesic to a neighboring one. As we showed above, this vector obeys

$$\frac{DV^\mu}{d\tau} \equiv U^\nu \nabla_\nu V^\mu = B^\mu{}_\nu V^\nu, \tag{C.5}$$

and from equation (C.3), we find

$$B^\mu{}_\nu = \nabla_\nu U^\mu. \tag{C.6}$$

We can interpret equation (C.6) as follows: the tensor $B_{\mu\nu}$ measures the deviation of the vector V^μ from being parallel transported along the geodesic (thus, along the τ direction). Since we are considering an entire congruence, and not just a one parameter family of curves as we did previously, this tensor proves to be very useful. We can think of three normal vectors, orthogonal to the timelike geodesics. Since we are working in a four dimensional spacetime, these normal vectors obviously exist. The tensor $B_{\mu\nu}$, thus the failure of these vectors to be parallel transported, will then tell us the behavior of nearby geodesics of the congruence. Put in other words, we could consider a sphere of particles centered at some point. To be able to describe the evolution of these particles with respect to the central geodesic, all we need is $B_{\mu\nu}$.

In this paper, null congruences are of special importance. Therefore, we leave the timelike case and have a more detailed look at the null congruences. Different from the timelike case, we cannot follow the evolution of vectors in a three dimensional subspace normal to the tangent field, since the tangent vector of a null curve, $k^\mu = \frac{dx^\mu}{d\lambda}$, is also normal to itself: $k^\mu k_\mu = 0$. The strategy will be to consider the evolution of vectors in a two dimensional subspace of *spatial* vectors normal to the null tangent vector field k^μ.

Of course, there is no Lorentz covariant way of uniquely defining these spatial vectors. Let's now introduce an auxiliary null vector, l^μ, which points in the opposite spatial direction to k^μ, and is normalized as follows:

$$l^\mu l_\mu = 0, \quad l^\mu k_\mu = -1 \tag{C.7}$$

Furthermore, we require the auxiliary vector to be parallel-transported,

$$k^\mu \nabla_\mu l^\nu = 0. \tag{C.8}$$

We remark that the auxiliary vector is not unique, because the opposite spatial direction is frame-dependent. We can now define the two-dimensional space of normal vectors, $T_\perp$, as the collection of vectors V^μ that are orthogonal to both k^μ and l^μ:

$$T_\perp = \{V^\mu \mid V^\mu k_\mu = 0, \quad V^\mu l_\mu = 0\}\,. \tag{C.9}$$

At each point p the space $T_\perp$ is a subspace of T_pM corresponding to the vectors that are spatially normal to k^μ. We can then introduce a projection tensor, which projects any vector of T_pM in $T_\perp$:

$$Q_{\mu\nu} = g_{\mu\nu} + k_\mu l_\nu + k_\nu l_\mu. \tag{C.10}$$

Indeed, the tensor $Q_{\mu\nu}$ will act as the metric for vectors $V^\mu, W^\mu \in T_\perp$, and will annihilate anything proportional to k^μ or l^μ. The failure of a normal deviation vector V^μ to be parallel transported along a null geodesic is determined by the tensor $B^\mu{}_\nu = \nabla_\nu k^\mu$, just as we derived in the timelike case,

$$\frac{DV^\mu}{d\lambda} \equiv k^\nu \nabla_\nu V^\mu = B^\mu{}_\nu V^\nu \tag{C.11}$$

However, we can manipulate equation (C.11) as follows:

$$\begin{aligned}\frac{DV^\mu}{d\lambda} &= k^\nu \nabla_\nu V^\mu \\ &= k^\nu \nabla_\nu (Q^\mu{}_\rho V^\rho) \\ &= Q^\mu{}_\rho k^\nu \nabla_\nu V^\rho \\ &= Q^\mu{}_\rho B^\rho{}_\nu V^\nu \\ &= Q^\mu{}_\rho B^\rho{}_\nu Q^\nu{}_\sigma V^\sigma \\ &= \hat{B}^\mu{}_\sigma V^\sigma, \end{aligned} \tag{C.12}$$

where $\hat{B}^\mu{}_\sigma$ is the projected tensor. We have thus showed that it is sufficient to follow the evolution of this projected tensor, and not the full tensor, in order to describe the evolution of a null congruence. Let's decompose this projected tensor into a symmetric and antisymmetric part. Moreover, we will decompose the symmetric part further in a trace and trace-free part. It is obvious that the projected tensor $\hat{B}_{\mu\nu}$ lays in the normal subspace, and hence one can use $Q_{\mu\nu}$ to take the trace, since this projection tensor acts like the metric in the normal subspace. We write the decomposition as

$$\hat{B}_{\mu\nu} = \frac{1}{2}\theta Q_{\mu\nu} + \sigma_{\mu\nu} + \omega_{\mu\nu} \tag{C.13}$$

where we have introduced three quantities. The *expansion* θ of the congruence,

$$\theta = Q^{\mu\nu}\hat{B}_{\mu\nu} = \hat{B}^\mu{}_\mu, \tag{C.14}$$

which is just the trace of $\hat{B}_{\mu\nu}$. The expansion describes the change in volume described by the test particles around the central geodesic. It is a scalar quantity, which we expect it to be, since the expansion or contraction of the volume is described by a number. The *shear* $\sigma_{\mu\nu}$, given by

$$\sigma_{\mu\nu} = \hat{B}_{(\mu\nu)} - \frac{1}{2}\theta Q_{\mu\nu}, \tag{C.15}$$

is symmetric and traceless. It represents a distortion in the shape of the collection of test particles, e.g. from an initial sphere into an ellipsoid. The symmetry represents the fact that the elongation along e.g. the x-direction is the same as in the $(-\text{x})$-direction. The third quantity is the *twist* $\omega_{\mu\nu}$ given by

$$\omega_{\mu\nu} = \hat{B}_{[\mu\nu]}, \tag{C.16}$$

and is antisymmetric. This makes sense: the xy component, for example, describes a rotation about the z axis, while the yx component describes a rotation around the same axis but in the opposite sense. We can now investigate the evolution of a congruence by taking the covariant

derivative of the tensor $\hat{B}_{\mu\nu}$ along the path.

$$\begin{aligned}
\frac{D\hat{B}_{\mu\nu}}{d\lambda} &\equiv k^\sigma \nabla_\sigma \hat{B}_{\mu\nu} \\
&= k^\sigma \nabla_\sigma \left(Q^\alpha{}_\nu Q^\beta{}_\mu \nabla_\alpha k_\beta \right) \\
&= Q^\alpha{}_\nu Q^\beta{}_\mu k^\sigma \nabla_\sigma \nabla_\alpha k_\beta \\
&= Q^\alpha{}_\nu Q^\beta{}_\mu \left(k^\sigma \nabla_\alpha \nabla_\sigma k_\beta + k^\sigma R^\lambda{}_{\beta\alpha\sigma} k_\lambda \right) \\
&= Q^\alpha{}_\nu Q^\beta{}_\mu \left(\nabla_\alpha \left(k^\sigma \nabla_\sigma k_\beta \right) - \left(\nabla_\alpha k^\sigma \right) \left(\nabla_\sigma k_\beta \right) + R_{\lambda\beta\alpha\sigma} k^\lambda k^\sigma \right) \\
&= -\hat{B}_\nu{}^\sigma \hat{B}_{\mu\sigma} - Q^\alpha{}_\nu Q^\beta{}_\mu R_{\beta\lambda\alpha\sigma} k^\lambda k^\sigma
\end{aligned} \tag{C.17}$$

We can take now the trace of equation (C.17) to find an evolution for the expansion of null geodesics,

$$\frac{d\theta}{d\lambda} = -\frac{1}{2}\theta^2 - \sigma^{\mu\nu}\sigma_{\mu\nu} + \omega^{\mu\nu}\omega_{\mu\nu} - R_{\mu\nu}k^\mu k^\nu \tag{C.18}$$

The first three terms are obtained by decomposing the sum $\hat{B}^{\mu\sigma}\hat{B}_{\mu\sigma}$ in terms of symmetric and anti-symmetric parts of the tensor $\hat{B}_{\mu\nu}$ and applying the definitions of equations (C.14) to (C.16). The last term follows by applying $Q^\alpha{}_\nu Q^{\nu\beta} = Q^{\alpha\beta} = g^{\alpha\beta} + k^\alpha l^\beta + l^\alpha k^\beta$, where only the term with the metric will not vanish due to the antisymmetric properties of the Riemann tensor. Equation (C.18) is called the Raychaudhuri's equation. It can be shown that it is completely independent of the choice of the auxiliary vector l^μ.

Appendix D

Conformal Diagrams

Conformal diagrams, or Penrose diagrams, are a way to visualize a spacetime with infinite size in space and/or time in a finite diagram, without loosing the causal relations. To find such a conformal diagrams, one starts from conformal transformations. These transformations are essentially like a local change of scale, and hence implemented by multiplying the metric by a spacetime-dependent (nonvanishing) function. The transformation takes the physical metric $g_{\mu\nu}$ to an unphysical metric $\tilde{g}_{\mu\nu}$, $\tilde{g}_{\mu\nu} = \omega^2(x)g_{\mu\nu}$, where $\omega(x)$ is a non-vanishing function. The critical point is that null curves are left invariant by conformal transformations. Indeed, it can easily be shown that if we have a null curve with respect to $g_{\mu\nu}$, it will also be a null curve with respect to $\tilde{g}_{\mu\nu}$. An important consequence is that light cones are left invariant.

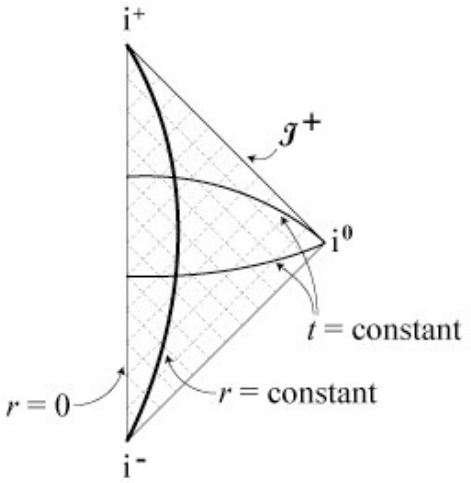

Figure D.1: The conformal diagram for Minkowski spacetime.

Hence, the causal structure (relation between past and future of events), is conserved with

conformal transformations. The main rules for a conformal diagram are the same as those of other spacetime diagrams. A conformal diagram will have a 'timelike' coordinate, which goes up, and a 'radial' coordinate. Light rays travel at 45 degrees. The differences lay in the fact that we aim for coordinates in which infinity is only a finite coordinate value away (so that the structure of the entire spacetime is immediately apparant), and that almost every point on the diagram represents a sphere.

Bibliography

[1] R. Bousso. The holographic principle. *Rev. Mod. Phys.*, 74(2):825, 2002.

[2] R. Bousso, B. Freivogel, and S. Leichenauer. Saturating the holographic entropy bound. *Phys. Rev.*, D82(084024), 2010.

[3] C.E. Shannon. Information in the Holographic Universe. *Bell System Technical Journal*, vol. 27:379–423 and 623–656, 1948.

[4] E.T. Jaynes. Information Theory and Statistical Mechanics. *The Physical Review*, 106(4):620–630, 1957.

[5] J.D. Bekenstein. A mathematical theory of communication. *Scientific American*, 289(2):61, 2003.

[6] R. Bousso. A covariant entropy conjecture. *JHEP*, 07(004), 1999.

[7] R. Bousso. Holography in general space-times. *JHEP*, 06(028), 1999.

[8] S.M. Carroll. *Spacetime and geometry.* Pearson, 2004.

[9] G.F.R Ellis and H. van Elst. Cosmological models. *Mathematical and Physical Sciences*, 541:1 , 116, 1999.

[10] J.D. Bekenstein. A universal upper bound on the entropy to energy ratio for bounded systems. *Phys. Rev. D*, 289:287, 1981.

[11] N. Kaloper and A. Linde. Cosmology vs. holography. *hep-th/9904120*, 289, 1999.

[12] W. Fischler and L. Susskind. Holography and cosmology. *hep-th/9806039*, 1998.

[13] S. Gao and J. Lemos. The covariant entropy bound in gravitational collapse. *hep-th/0403284v2*, 2004.